Tumor-selective adenoviral-mediated GFP genetic labeling of human cancer in the live mouse reports future recurrence after resection

Hiroyuki Kishimoto,[1-3] Ryoichi Aki,[1,2] Yasuo Urata,[4] Michael Bouvet,[2] Masashi Momiyama,[1,2] Noriaki Tanaka,[3] Toshiyoshi Fujiwara[3] and Robert M. Hoffman[1,2,*]

[1]AntiCancer, Inc.; [2]Department of Surgery; University of California at San Diego; San Diego, CA USA; [3]Division of Surgical Oncology; Department of Surgery; Okayama University Graduate School of Medicine; Dentistry and Pharmaceutical Sciences; Okayama, Japan; [4]Oncolys BioPharma, Inc.; Tokyo, Japan

We have previously developed a telomerase-specific replicating adenovirus expressing GFP (OBP-401), which can selectively label tumors in vivo with GFP. Intraperitoneal (i.p.) injection of OBP-401 specifically labeled peritoneal tumors with GFP, enabling fluorescence visualization of the disseminated disease and real-time fluorescence surgical navigation. However, technical problems of removing all cancer cells still remain, even with fluorescence-guided surgery. In this study, we report that in vivo OBP-401 labeling of tumors with GFP before fluorescence-guided surgery reports cancer recurrence after surgery. Recurrent tumor nodules brightly expressed GFP, indicating that initial OBP-401-GFP labeling of peritoneal disease was genetically stable such that proliferating residual cancer cells still express GFP. In situ tumor labeling with a genetic reporter has important advantages over antibody and other non-genetic labeling of tumors, since residual disease remains labeled during recurrence and can be further resected under fluorescence guidance.

Introduction

Green fluorescent protein (GFP) serves as a very bright genetic reporter to detect metastatic cancer in mouse models.[1-3] Initially, cancer cells were transduced in vitro with GFP using various types of genetic vectors and then implanted in mouse models. Potential clinical application of GFP became possible when it was demonstrated that retroviruses containing GFP could label disseminated cancer in situ in mouse models.[4] Subsequently, selective in vivo GFP labeling of tumors was performed with OBP-401, a replicating adenovirus[5,6] that contains a replication cassette with the human telomerase reverse transcriptase (hTERT) promoter driving the expression of the viral *E1* genes, and the inserted *GFP* gene. Virus replication and hence *GFP* gene expression occur only in the presence of an active telomerase, i.e., in malignant tissue.[6] The OBP-401 virus was first tested by injection directly into HT-29 human colon tumors, orthotopically implanted into the rectum in BALB/c *nu/nu* mice. Subsequent para-aortic lymph node metastasis was observed by laparotomy under fluorescence.[6] We then developed a major enhancement of cancer surgical navigation in orthotopic mouse models of cancer, using in vivo selective fluorescent tumor labeling with OBP-401 GFP. Bright GFP fluorescence clearly illuminated the tumor boundaries and facilitated detection of the smallest disseminated disease lesions.[7]

Fluorescence-guided surgical navigation with tumors labeled in vivo with OAP-401 GFP was demonstrated in nude mouse models that represent difficult surgical challenges for the resection of widely disseminated cancer. HCT-116, a model of intraperitoneal disseminated human colon cancer, was labeled by virus injection into the peritoneal cavity. A549, a model of pleural dissemination of human lung cancer, was labeled by OBP-401 virus administered into the pleural cavity. Only the malignant tissue fluoresced brightly in both models. Further, we showed that OBP-401 could visualize liver metastases by tumor-specific expression of the GFP gene after portal venous or i.v. administration. Selective metastatic tumor labeling with GFP and killing by systemic administration of telomerase-dependent adenoviruses suggesting that liver metastasis is also a candidate for fluorescence-guided surgery.[8]

However, even fluorescence-guided surgery may still result in residual disease. The present report demonstrates proliferating residual disease remains stably labeled with OBP-401 GFP and is readily detected for further resection, suggesting that genetic-reporter labeling of tumors has advantages over non-genetic labeling of tumors for fluorescence-guided surgery.
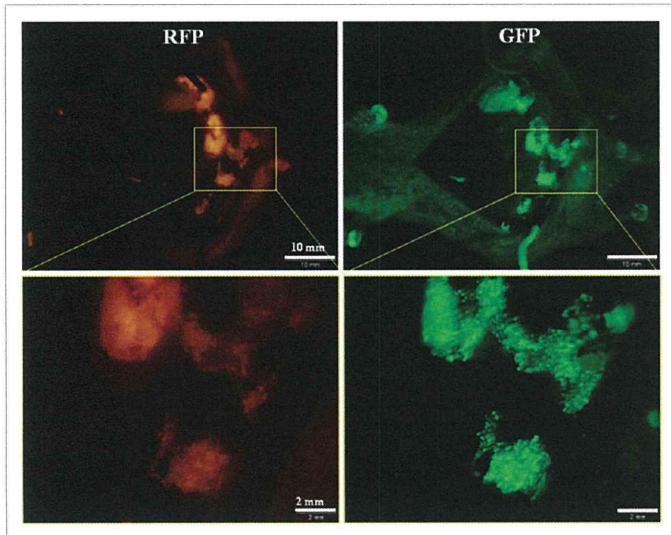
Results and Discussion

Labeling peritoneal carcinomatosis with OBP-401-GFP. Peritoneal carcinomatosis was induced in the abdominal cavity of nude mice by i.p. implantation of HCT-116-RFP human colorectal cancer cells. Twelve days after implantation, 1×10^8 PFU

Figure 1. In situ genetic labeling of disseminated peritoneal carcinomatosis. Red fluorescence indicates HCT-116-RFP-expressing disseminated nodules (left). Peritoneal disseminated HCT116-RFP cells were labeled by GFP after i.p. injection of OBP-401 (right). Fluorescence imaging revealed co-localization of red and green fluorescence.

OBP-401 were injected intraperitoneally. Disseminated HCT-116-RFP nodules expressed GFP fluorescence induced by OBP-401 as well as the endogenous RFP fluorescence when imaged 5 d later (**Fig. 1**). RFP fluorescence was essentially coincident with that of GFP, indicating that i.p. injection of OBP-401 efficiently labeled disseminated tumors with GFP.

Stability of OBP-401-GFP expression in tumors. In order to determine stability of GFP expression in OBP-401 labeled tumors, HCT-116-RFP tumors were collected by peritoneal lavage from the abdominal cavity of mice 5 d after OBP-401 administration, put into culture in RPMI 1640 medium supplemented with 10% FBS and observed over time. Eight days after plating (13 d after viral administration), cancer cell colonies expressed both RFP and GFP (**Fig. 2**). The stability of GFP expression in OBP-401 labeled tumor cells suggests the potential of OBP-401 GFP labeling to detect recurrent tumors after attempted resection.

Fluorescence-guided resection of disseminated peritoneal tumors labeled with OBP-401 GFP. Five days after OBP-401 administration to mice with i.p. HCT-116, laparotomy was performed with the intent to remove all the intra-abdominal cancer using fluorescence-guided navigation under ketamine anesthesia (**Fig. 3A and B**). OBP-401 labeling and imaging made disseminated cancer nodules visible by GFP fluorescence, and complete resection was attempted (**Fig. 3C–E**). Tumors were efficiently resected, including those not visible under bright light, as we have previously reported in references 7 and 8.

In vivo detection of recurrent OBP-402-GFP labeled tumors after fluorescence-guided surgery. Tumors still recurred after attempted complete resection with fluorescence-guided surgery as visualized by GFP expression (**Fig. 4**). This result demonstrates that OBP-401 GFP labeling of peritoneal disseminated disease

enables detection of tumor recurrence after fluorescence-guided surgery. Thus, OBP-401-GFP labeling is genetically stable and therefore proliferating residual disease continues to express GFP.

Tsien's laboratory has developed a method to label and visualize tumors during surgery using activatable cell-penetrating peptides (ACPPs), in which the fluorescently-labeled, polycationic cell-penetrating peptide (CPP) is coupled via a cleavable linker to a neutralizing peptide. Upon exposure to proteases expressed by tumors, the linker is cleaved, dissociating the inhibitory peptide and allowing the CPP to bind to and enter tumor cells. Animals whose tumors were resected with ACPPD guidance had better long-term tumor-free survival and overall survival than animals whose tumors were resected with traditional brightfield illumination only.[9]

Another approach to tumor labeling and fluorescence-guided surgery is with the use of labeled tumor-specific antibodies. A monoclonal antibody specific for CA19-9 was conjugated to a green fluorophore and delivered to tumor-bearing mice as a single intravenous (IV) dose. Intravital fluorescence imaging was used to localize metastatic pancreatic cancer in orthotopic mouse models 24 h after antibody administration. Using fluorescence imaging, the primary tumor was clearly visible at laparotomy, as were small metastases in the liver and spleen and on the peritoneum. The metastatic tumors, which were nearly impossible to see using standard brightfield imaging, demonstrated clear fluorescence under LED light excitation.[10]

We have also previously investigated the use of fluorophore-labeled anti-carcinoembryonic antigen (CEA) monoclonal antibody to aid in cancer visualization in nude mouse models of human colorectal and pancreatic cancer. Anti-CEA was conjugated with a green fluorophore. Subcutaneous, orthotopic primary and metastatic human pancreatic and colorectal tumors were easily visualized with fluorescence imaging after administration of conjugated anti-CEA. The fluorescence signal was detectable 30 min after systemic antibody delivery and remained present for 2 weeks, with minimal in vivo photobleaching after exposure to standard operating room lighting. Fluorescent anti-CEA administration improved ability to resect the labeled tumors under fluorescence guidance.[11]

Neither the ACPP nor labeled monoclonal antibodies, described above, involves genetic labeling of cancer cells, and thus recurrence would therefore not be detectable. In the present study, we selectively and efficiently labeled tumors with a genetic reporter, GFP, using a telomerase dependent adenovirus OBP-401. We demonstrated that tumors recurred after fluorescence-guided surgery and maintained GFP expression. Therefore, the detection of recurrence and future metastasis is possible with OBP-401 GFP labeling, since recurrent cancer cells stably express GFP, which is not possible with non-genetic labeling of tumors.

In clinical studies performed with OBP-401, circulating tumor cells (CTC) obtained from cancer patients were labeled with OBP-401 GFP ex vivo. OBP-401-GFP labeling greatly increased the detection of CTC.[12] Other targets for in vivo GFP labeling could include, for example, breast cancer emboli.[13] Specific labeling by GFP of cancer stem cells is also a promising approach.[14]
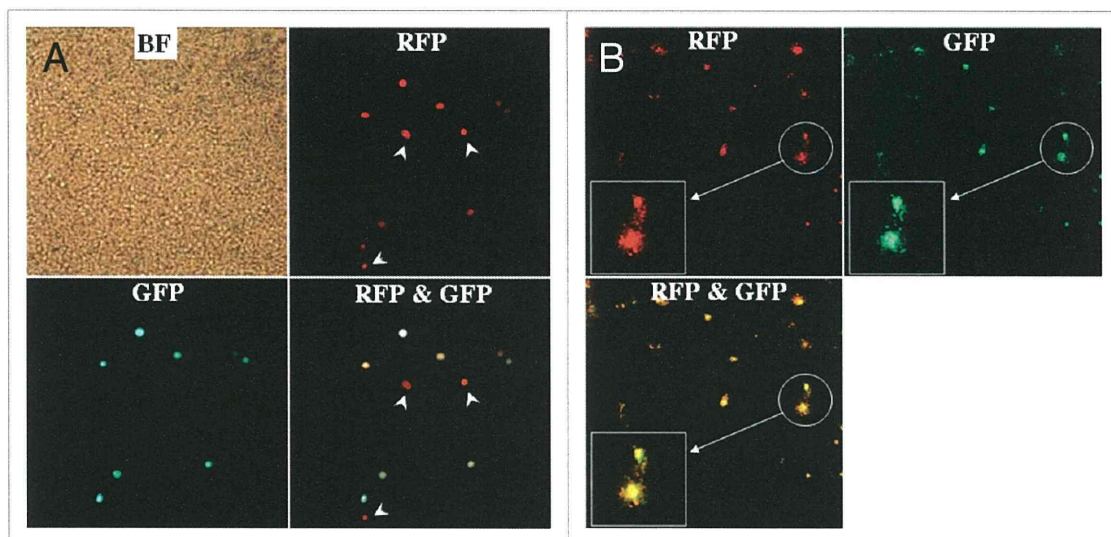
Figure 2. Genetic labeling of microscopic tumors. Cells collected by peritoneal lavage from the abdominal cavity of mice 5 d after OBP-401 treatment were plated and cultured with RPMI 1640 medium supplemented with 10% FBS. (A) Plating cells in the peritoneal lavage fluid (5 d after viral administration). Most RFP-expressing cancer cells expressed GFP fluorescence induced by OBP-401 as well, x200 magnification. White arrows: cells unlabeled with GFP. (B) 8 d after plating (i.e., 13 d after viral administration). Cancer cell colonies expressing RFP were observed in the culture dish under fluorescence microscopy. The cancer cells also expressed GFP induced by OBP-401. x40 magnification. Boxes highlight colonies indicated by white circles. Original magnification x100.
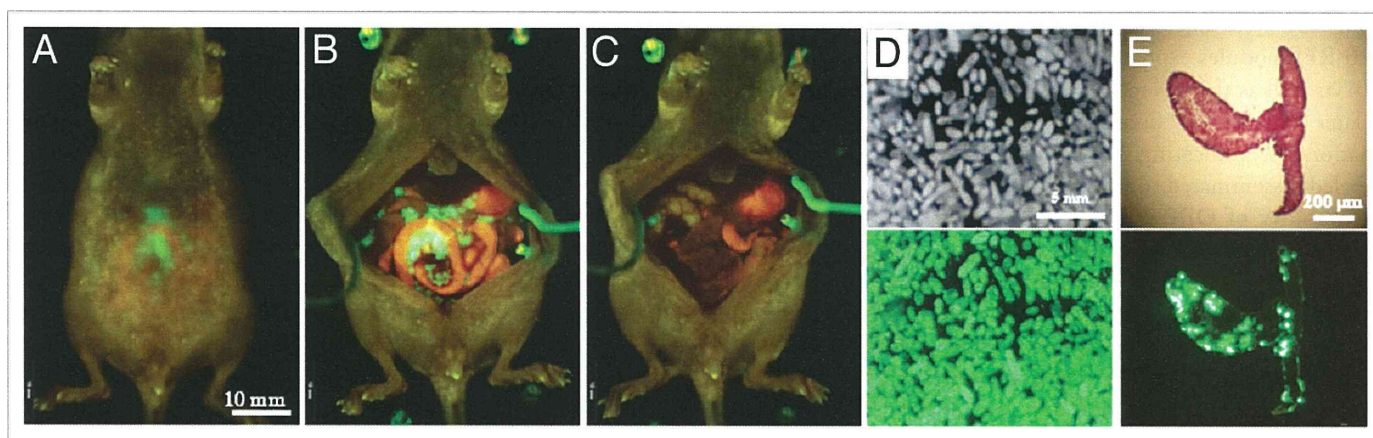
Figure 3. Fluorescence-guided resection of tumors labeled with GFP in situ. (A) Peritoneal disseminated nodules were labeled by GFP expression 5 d after OBP-401 virus administration. (B) Laparotomy was performed. (C) Disseminated nodules labeled with GFP were removed under GFP-guided surgical navigation. (D) Disseminated nodules removed under GFP-guided navigation. Top, bright field observation; bottom, fluorescent detection. (E) Section of disseminated nodules. Top, H&E section; bottom, frozen section with fluorescence detection.

Labeling of cancer stem cells is especially important, since at least some stem cells can now be imaged non-invasively.[15] The present report suggests the clinical potential of OBP-401 GFP labeling to improve the surgical outcome of cancer.

Materials and Methods

Recombinant adenovirus. Telomerase-specific replication-selective adenovirus OBP-401, containing the *GFP* gene under the control of the CMV promoter with the hTERT promoter driving the *E1A* and *E1B* genes, was constructed and produced as previously described in references 5 and 6.

Cell culture. The human colorectal cancer cell line HCT-116 was cultured in RPMI 1640 medium supplemented with 10% FBS.

Production of red fluorescent protein (RFP) retroviral vector. For RFP retrovirus production, the *Hind*III/*Not*I fragment from pDsRed2 (Clontech), containing the full-length RFP cDNA, was inserted into the *Hind*III/*Not*I site of pLNCX2 (Clontech) containing the neomycin-resistance gene. PT67, an NIH3T3-derived packaging cell line (Clontech) expressing the viral envelope, was cultured in DMEM supplemented with 10% FBS. For vector production, PT67 packaging cells, at 70% confluence, were incubated with a precipitated mixture of LipofectAMINE reagent

41
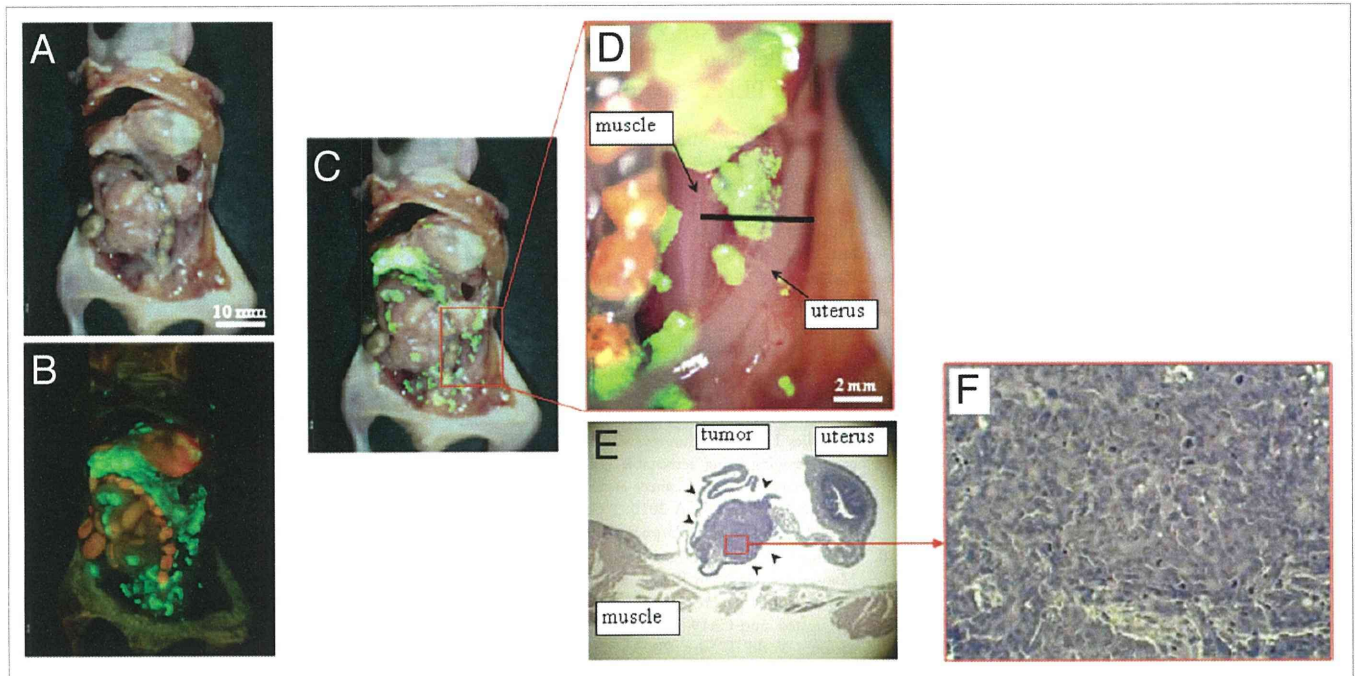
Figure 4. In vivo detection of recurrent tumors after fluorescence-guided surgery. (A) Brightfield observation several weeks after fluorescence-guided surgery of OBP-401 GFP-labeled tumors. Disseminated disease re-emerged. (B) Fluorescence observation of field observed by brightfield in (A). (C) Merge of (A and B). The red box outlines a region of (D) below. (D) Detail of the boxed region of (C). Black line indicates the direction of cross-sections. (E) Histologic sections stained with H&E showing that GFP-labeled lesions are recurrent tumor tissues (arrow heads). x40 magnification. (F) Detail of the boxed region of (E). x200 magnification.

(Life Technologies) and saturating amounts of pLNCX2-DsRed2 plasmid for 18 h. Fresh medium was replenished at this time. The cells were examined by fluorescence microscopy 48 h post-transduction. For selection of a clone producing high amounts of RFP retroviral vector (PT67-DsRed2), the cells were cultured in the presence of 200 to 1,000 µg/ml G418 (Life Technologies) for 7 d. The isolated packaging cell clone was termed PT67-DSRed2.[16]

RFP gene transduction of cancer cells. For RFP gene transduction, cancer cells were incubated with a 1:1 precipitated mixture of retroviral supernatants of PT67 cells and RPMI 1640 containing 10% FBS for 72 h. Fresh medium was replenished at this time. Tumor cells were harvested with trypsin/EDTA 72 h post-transduction and subcultured at a ratio of 1:15 into selective medium, which contained 200 µg/ml G418. To select brightly fluorescent cells, the level of G418 was increased up to 800 µg/ml in a stepwise manner. RFP-expressing cancer cells were isolated with cloning cylinders using trypsin/EDTA and were amplified by conventional culture methods in the absence of selective agent.[16]

Mice. Athymic nude mice were kept in a barrier facility under HEPA filtration and fed with autoclaved laboratory rodent diet. All animal studies were conducted in accordance with the principals and procedures outlined in the National Institute of Health Guide for the Care and Use of Laboratory Animals under Assurance Number A3873-1. All animal procedures were performed under anesthesia using s.c. administration of a ketamine mixture (10 µl ketamine HCL, 7.6 µl xylazine, 2.4 µl acepromazine maleate and 10 µl PBS).

In vivo fluorescence imaging. An Olympus OV100 Small Animal Imaging System (Olympus Corp., Tokyo, Japan) with macro and micro optics was used.[17] High-resolution images directly captured on a PC were processed and analyzed with the use of Adobe Photoshop Elements 4.0 software (Adobe).

Peritoneal carcinomatosis model with HCT-116 human colon cancer cells implanted in nude mice. Nude mice were intraperitoneally (i.p.) injected either with HCT-116 or HCT-116-RFP human colon cancer cells at a density of 3 x 10⁶ in 200 µl PBS. Twelve days after tumor cell inoculation, mice were injected i.p. with OBP-401 at a dose of 1 x 10⁸ PFU in 200 µl PBS. Five days after virus injection, the abdominal cavity was examined by fluorescence imaging, and mice were operated on with fluorescence guidance with the intent to resect all intra-abdominal tumor nodules under ketamine-induced anesthesia.

Collection of microscopic tumors from peritoneal lavage fluid of OBP-401 treated mice. Twelve days after nude mice were i.p. injected with HCT-116-RFP, 1 x 10⁸ PFU OBP-401 were injected intraperitoneally. Five days after virus injection, mice were instilled with 8 ml PBS intraperitoneally. The abdomen was gently massaged and the peritoneal fluid was carefully aspirated using a 22-gauge needle. Approximately 6 ml peritoneal lavage fluid (PLF) were obtained from most mice. After filtering the PLF with a 40 µm cell strainer (BD, Franklin Lakes, NJ) in order to collect only microscopic tumors and/or cancer cells in the abdominal cavity, 3 ml of PLF were cultured on 6-well tissue culture plates. After incubation for 1 h, supernatants were carefully aspirated and 3 ml RPMI 1640 medium, containing 10% FBS,

were added to each well. The cells were further incubated at 37°C in a humidified atmosphere of 5% CO_2 and observed under fluorescence microscopy at day 0 and day 8 after collection of PLF.

References

1. Chishima T, Miyagi Y, Wang X, Yamaoka H, Shimada H, Moossa AR, et al. Cancer invasion and micrometastasis visualized in live tissue by green fluorescent protein expression. Cancer Res 1997; 57:2042-7; PMID: 9158003.

2. Yang M, Baranov E, Jiang P, Sun FX, Li XM, Li L, et al. Whole-body optical imaging of green fluorescent protein-expressing tumors and metastases. Proc Natl Acad Sci USA 2000; 97:1206-11; PMID: 10655509; DOI: 10.1073/pnas.97.3.1206.

3. Hoffman RM. The multiple uses of fluorescent proteins to visualize cancer in vivo. Nat Rev Cancer 2005; 5:796-806; PMID: 16195751; DOI: 10.1038/nrc1717.

4. Hasegawa S, Yang M, Chishima T, Miyagi Y, Shimada H, Moossa AR, et al. In vivo tumor delivery of the green fluorescent protein gene to report future occurrence of metastasis. Cancer Gene Ther 2000; 7:1336-40; PMID: 11059691; DOI: 10.1038/sj.cgt.0237.

5. Fujiwara T, Kagawa S, Kishimoto H, Endo Y, Hioki M, Ikeda Y, et al. Enhanced antitumor efficacy of telomerase-selective oncolytic adenoviral agent OBP-401 with docetaxel: preclinical evaluation of chemovirotherapy. Int J Cancer 2006; 119:432-40; PMID: 16477640; DOI: 10.1002/ijc.21846.

6. Kishimoto H, Kojima T, Watanabe Y, Kagawa S, Fujiwara T, Uno F, et al. In vivo imaging of lymph node metastasis with telomerase-specific replication-selective adenovirus. Nat Med 2006; 12:1213-9; PMID: 17013385; DOI: 10.1038/nm1404.

7. Kishimoto H, Zhao M, Hayashi K, Urata Y, Tanaka N, Fujiwara T, et al. In vivo internal tumor illumination by telomerase-dependent adenoviral GFP for precise surgical navigation. Proc Natl Acad Sci USA 2009; 106:14514-7; PMID: 19706537; DOI: 10.1073/pnas.0906388106.

8. Kishimoto H, Urata Y, Tanaka N, Fujiwara T, Hoffman RM. Selective metastatic tumor labeling with green fluorescent protein and killing by systemic administration of telomerase-dependent adenoviruses. Mol Cancer Ther 2009; 8:3001-8; PMID: 19887549; DOI: 10.1158/1535-7163.MCT-09-0556.

9. Nguyen QT, Olson ES, Aquilera TA, Jiang T, Scadeng M, Ellies LG, et al. Surgery with molecular fluorescence imaging using activatable cell-penetrating peptides decreases residual cancer and improves survival. Proc Natl Acad Sci USA 2010; 107:4317-22; PMID: 20160097; DOI: 10.1073/pnas.0910261107.

10. McElroy M, Kaushal S, Luiken G, Talamini MA, Moossa AR, Hoffman RM, et al. Imaging of primary and metastatic pancreatic cancer using a fluorophore-conjugated anti-CA19-9 antibody for surgical navigation. World J Surg 2008; 32:1057-66; PMID: 18264829; DOI: 10.1007/s00268-007-9452-1.

11. Kaushal S, McElroy MK, Luiken GA, Talamini MA, Moossa AR, Hoffman RM, et al. Fluorophore-conjugated anti-CEA antibody for the intraoperative imaging of pancreatic and colorectal cancer. J Gastrointest Surg 2008; 12:1938-50; PMID: 18665430; DOI: 10.1007/s11605-008-0581-0.

12. Kojima T, Hashimoto Y, Watanabe Y, Kagawa S, Uno F, Kuroda S, et al. A simple biological imaging system for detecting viable human circulating tumor cells. J Clin Invest 2009; 119:3172-81; PMID: 19729837; DOI: 10.1172/JCI38609.

13. Mahooti S, Porter K, Alpaugh ML, Ye Y, Xiao Y, Jones S, et al. Breast carcinomatous tumoral emboli can result from encircling lymphovasculogenesis rather than lymphovascular invasion. Oncotarget 2010; 1:131-47; PMID: 21297224.

14. Runck LA, Kramer M, Ciraolo G, Lewis AG, Guasch G. Identification of epithelial label-retaining cells at the transition between the anal canal and the rectum in mice. Cell Cycle 2010; 9:3039-45; PMID: 20647777; DOI: 10.4161/cc.9.15.12437.

15. Uchugonova A, Hoffman RM, Weinigel M, Koenig K. Watching stem cells in the skin of living mice noninvasively. Cell Cycle 2011; 10:2017-20; PMID: 21558804; DOI: 10.4161/cc.10.12.15895.

16. Yamamoto N, Yang M, Jiang P, Xu M, Tsuchiya H, Tomita K, et al. Real-time imaging of individual fluorescent-protein color-coded metastatic colonies in vivo. Clin Exp Metastasis 2003; 20:633-8; PMID: 14669794; DOI: 10.1023/A:1027311230474.

17. Yamauchi K, Yang M, Jiang P, Xu M, Yamamoto N, Tsuchiya H, et al. Development of real-time subcellular dynamic multicolor imaging of cancer-cell trafficking in live mice with a variable-magnification whole mouse imaging system. Cancer Res 2006; 66:4208-14; PMID: 16618743; DOI: 10.1158/0008-5472.CAN-05-3927.

SHORT COMMUNICATION

A simple detection system for adenovirus receptor expression using a telomerase-specific replication-competent adenovirus

T Sasaki[1], H Tazawa[2,3], J Hasei[1], S Osaki [1], T Kunisada[1,4], A Yoshida[1], Y Hashimoto[3], S Yano[3], R Yoshida[3], S Kagawa[3], F Uno[3], Y Urata[5], T Ozaki[1] and T Fujiwara[3]

Adenovirus serotype 5 (Ad5) is frequently used as an effective vector for induction of therapeutic transgenes in cancer gene therapy or of tumor cell lysis in oncolytic virotherapy. Ad5 can infect target cells through binding with the coxsackie and adenovirus receptor (CAR). Thus, the infectious ability of Ad5-based vectors depends on the CAR expression level in target cells. There are conventional methods to evaluate the CAR expression level in human target cells, including flow cytometry, western blotting and immunohistochemistry. Here, we show a simple system for detection and assessment of functional CAR expression in human tumor cells, using the green fluorescent protein (GFP)-expressing telomerase-specific replication-competent adenovirus OBP-401. OBP-401 infection induced detectable GFP expression in CAR-expressing tumor cells, but not in CAR-negative tumor cells, nor in CAR-positive normal fibroblasts, 24 h after infection. OBP-401-mediated GFP expression was significantly associated with CAR expression in tumor cells. OBP-401 infection detected tumor cells with low CAR expression more efficiently than conventional methods. OBP-401 also distinguished CAR-positive tumor tissues from CAR-negative tumor and normal tissues in biopsy samples. These results suggest that GFP-expressing telomerase-specific replication-competent adenovirus is a very potent diagnostic tool for assessment of functional CAR expression in tumor cells for Ad5-based antitumor therapy.

Gene Therapy advance online publication, 12 January 2012; doi:10.1038/gt.2011.213

Keywords: oncolytic virus; adenovirus; telomerase; sarcoma; GFP

INTRODUCTION

Adenovirus serotype 5 (Ad5) is widely and frequently used as an effective vector in cancer gene therapy and oncolytic virotherapy.[1–3] Adenovirus-mediated transgene transduction is a highly efficient method for induction of ectopic transgene expression in tumor cells.[1,2] The p53 tumor suppressor gene, which is a potential therapeutic transgene that may induce a very strong antitumor effect, has been transduced into tumor cells using a replication-deficient adenovirus vector (Ad-p53, Advexin, Intorgen Therapeutics, Inc., Austin, TX, USA), and Ad-p53 has been reported to induce an antitumor effect in clinical studies.[4–7] Recently, an Ad5-based replication-competent oncolytic adenovirus has been developed as a promising anticancer reagent for induction of tumor-specific cell lysis.[8,9] Ad5-based vectors infect human target cells through binding with the coxsackie and adenovirus receptor (CAR).[10] Thus, the infection efficiency of Ad5-based vectors mainly depends on the CAR expression level in tumor tissues.[11–17] Increased CAR expression has been frequently shown in tumor cells in various organs such as the brain,[18] thyroid,[19] esophagus,[20] gastrointestinal tract,[21] prostate,[14] bone and soft tissues.[22–24] However, tumor cells often show reduced CAR expression following tumor progression.[18,21,25,26] Decreased CAR expression has also been shown in tumor tissues after repeated injection of Ad-p53.[27,28] It is therefore necessary to assess the CAR expression level of target tumor tissues before and after Ad5-based cancer gene therapy and oncolytic virotherapy.

There are some conventional methods for evaluation of the CAR expression level in tumor tissues, such as flow cytometry, immunohistochemistry, western blotting and reverse transcription (RT)-PCR . Flow cytometry is mainly used to detect CAR-positive human tumor cell lines.[13,24,28,29] Immunohistochemistry is frequently used to assess CAR expression in various human tumor tissues.[11,14,20,23,25] Western blotting is usually performed to confirm the expression of many types of proteins including CAR in molecular biological experiments. Quantitative RT-PCR is also a useful method for evaluation of the mRNA expression of CAR.[18,22] Although these conventional methods can detect CAR expression in tumor tissues, it still remains unclear whether Ad5-based vectors really infect target tumor cells through binding with the CAR that is detected using conventional methods. Therefore, the development of a novel method for assessment of the level of expression of functional CAR in tumor tissues, which is what the Ad5-based vectors really bind, is required for Ad5-based anticancer therapy.

We previously developed a telomerase-specific replication-competent adenovirus OBP-301 (Telomelysin, Oncolys BioPharma, Inc., Tokyo, Japan) that drives the E1A and E1B genes under the human telomerase reverse transcriptase (hTERT) promoter.[8,29–31] OBP-301 infects both normal and tumor cells that express CAR, but replicates only in CAR-positive tumor cells in a telomerase-dependent manner. Furthermore, we recently generated a green fluorescent protein (GFP)-expressing telomerase-specific replication-

competent adenovirus OBP-401, which induces ectopic GFP expression in tumor cells, but not in normal cells.[32] OBP-401 infection efficiently induces GFP expression in metastatic tumor cells at regional lymph nodes[32] and liver,[33] circulating tumor cells in blood flow[34] and disseminated tumor cells in the abdominal cavity.[35] These results suggest that OBP-401 is a highly sensitive tool for the detection of tumor cells. Furthermore, Ad5-based OBP-401 would also be useful for induction of GFP expression in CAR-positive tumor cells, but not in CAR-negative tumor cells.

In the present study, we evaluated whether induction of GFP expression by OBP-401 infection is associated with CAR expression in tumor cells. OBP-401-mediated GFP induction was further examined in xenograft tumor tissues that have different levels of CAR expression and in surrounding normal tissues.

RESULTS AND DISCUSSION

Assessment of an OBP-401 infection protocol for the detection of CAR-positive tumor cells

We recently demonstrated that the level of CAR expression that was detected using flow cytometry was significantly associated with OBP-301-mediated cytopathic activity in human bone and soft tissue sarcoma cells.[29] Furthermore, OBP-401 infection has been shown to induce GFP expression 24 h after infection of human sarcoma cells.[34] To evaluate whether GFP expression that is induced by OBP-401 infection is associated with CAR expression in tumor cells, we used three human sarcoma cell lines (OST, NMFH-1 and OUMS-27) that have different levels of CAR expression, as previously reported.[29] Flow cytometric analysis confirmed that OST cells showed detectable CAR expression, whereas cells of the NMFH-1 and OUMS-27 sarcoma cell lines had no detectable CAR expression (Figure 1a).

To determine suitable conditions for OBP-401 infection in order to detect CAR-positive tumor cells, OST sarcoma cells were infected with OBP-401 at multiplicity of infections (MOIs) of 1, 10 and 100 plaque-forming units (PFU) per cell over 24 h (Figure 1b and c). Twelve hours after infection, only OBP-401 infection at an MOI of 100 had induced GFP expression in all of the OST cells. Twenty-four hours after infection, OBP-401 infection at MOIs of 10 and 100 had induced ectopic GFP expression in all of the OST cells, whereas OBP-401 infection at an MOI of 1 had induced GFP expression in about 80% of the OST cells. These results indicate that OBP-401 infection at an MOI of greater than 10 is necessary to efficiently detect CAR-positive tumor cells 24 h after infection.

To subsequently determine a suitable condition for OBP-401 infection that would exclude CAR-negative tumor cells, the NMFH-1 and OUMS-27 sarcoma cells that do not express CAR were infected with OBP-401 at MOIs of 10 and 100 for 60 h (Figures 1d and e). NMFH-1 cells expressed GFP at 24 and 48 h after OBP-401 infection at MOIs of 100 and 10, respectively. In contrast, OUMS-27 cells exhibited no GFP expression after OBP-401 infection. To investigate the different GFP expression between these CAR-negative tumor cells, expression of integrins, $\alpha v\beta 3$ and $\alpha v\beta 5$, was further examined by flow cytometry. NMFH-1 cells showed twofold higher expression of integrin $\alpha v\beta 3$ compared with OUMS-27 cells, whereas $\alpha v\beta 5$ expression was similar in these cells (Supplementary Figure S1a). These results indicate that OBP-401 infection at an MOI of 10 for 24 h is a suitable protocol for distinguishing CAR-negative tumor cells from CAR-positive tumor cells, when CAR-negative tumor cells express integrin molecules.

Relationship between OBP-401-induced GFP expression and CAR expression

To evaluate whether OBP-401-induced GFP expression correlates with CAR expression in tumor cells, six human sarcoma cell lines

(OST, U2OS, NOS-10, MNNG/HOS, NMFH-1 and OUMS-27) and normal human lung fibroblasts (NHLF) cells that have different levels of CAR expression (Figure 1a and Supplementary Figure S1b) were infected with OBP-401 at an MOI of 10 for 24 h, and the GFP-positive cells in each cell type were analyzed under fluorescence microscopy (Figures 2a and b). OBP-401 infection-induced GFP expression from 12 h after infection and, after 24 h, more than 40% of all CAR-positive tumor cells (OST, U2OS, NOS-10 and MNNG/HOS) were detected as GFP-positive cells. However, no GFP-positive cells were detected in the CAR-negative tumor cells (NMFH-1, OUMS-27), or in the normal NHLF cells, 24 h after infection. Furthermore, OBP-401-mediated GFP induction in CAR-positive tumor cells was suppressed by blocking CAR proteins with anti-CAR antibody (Supplementary Figure S2). To assess the GFP expression level in all tumor and normal cells in a more quantitative manner, we quantified the level of GFP fluorescence in each cell type 24 h after infection using a fluorescence microplate reader (Figure 2c). We also quantified the level of CAR expression in these cells by calculating the mean fluorescence intensity in flow cytometric analysis (Figure 2d). GFP fluorescence was detected in CAR-positive tumor cells, but not in either CAR-negative tumor cells or in CAR-positive normal cells. There was a significant relationship between the CAR expression level and the GFP fluorescence level ($r = 0.885$; $P = 0.019$) (Figure 2e). These results indicate that OBP-401-mediated GFP expression is highly associated with CAR expression in tumor cells.

Comparison of the potential of OBP-401-mediated GFP induction and of conventional methods for CAR detection

To estimate the potential of OBP-401-mediated GFP induction for the detection of CAR-positive tumor cells, we compared the above protocol using OBP-401 with western blot analysis and immunocytochemistry. CAR expression was detected in OST, U2OS and NOS-10 sarcoma cells, but not in CAR-positive MNNG/HOS sarcoma cells, using western blot analysis (Supplementary Figure S3a). In contrast, only OST cells displayed a positive CAR signal using immunocytochemistry, whereas the CAR signal of the other three CAR-positive tumor cells was almost as weak as that from CAR-negative tumor cells (Supplementary Figure S3b). CAR expression was also not detected in CAR-positive NHLF cells by either western blot analysis or by immunocytochemistry. These results suggest that the GFP induction protocol using OBP-401 is more sensitive for the detection of CAR-positive tumor cells than conventional methods.

OBP-401-mediated GFP induction was detected in MNNG/HOS sarcoma cells that expressed a low level of CAR (Figure 2c), although neither western blot analysis nor immunocytochemistry detected CAR in these cells (Supplementary Figure S3). Furthermore, although conventional methods may be able to detect high CAR expression in tumor cells, whether the CAR expression that is detected by conventional methods is really functional for binding with Ad5-based vectors still remains unclear. In contrast, as OBP-401 is an Ad5-based vector that expresses a fluorescent *GFP* gene, OBP-401-induced GFP expression directly proves that the CAR that is expressed is functional for Ad5-based vector binding. Thus, the OBP-401-mediated GFP induction strategy is a potential diagnostic method that can efficiently and directly assess functional CAR expression in tumor cells.

OBP-401-mediated GFP induction in xenograft tumor and normal tissues with different CAR expression

Finally, to investigate the potential of the OBP-401-mediated method for the detection of CAR expression in tumor and normal tissues, we used this method to analyze CAR expression of human xenograft tumor tissues, that do or do not express CAR, as well as of surrounding normal muscle tissues, which have been previously shown to lose CAR expression.[36] CAR-positive OST sarcoma cells or CAR-negative OUMS-27 sarcoma cells were inoculated into nude
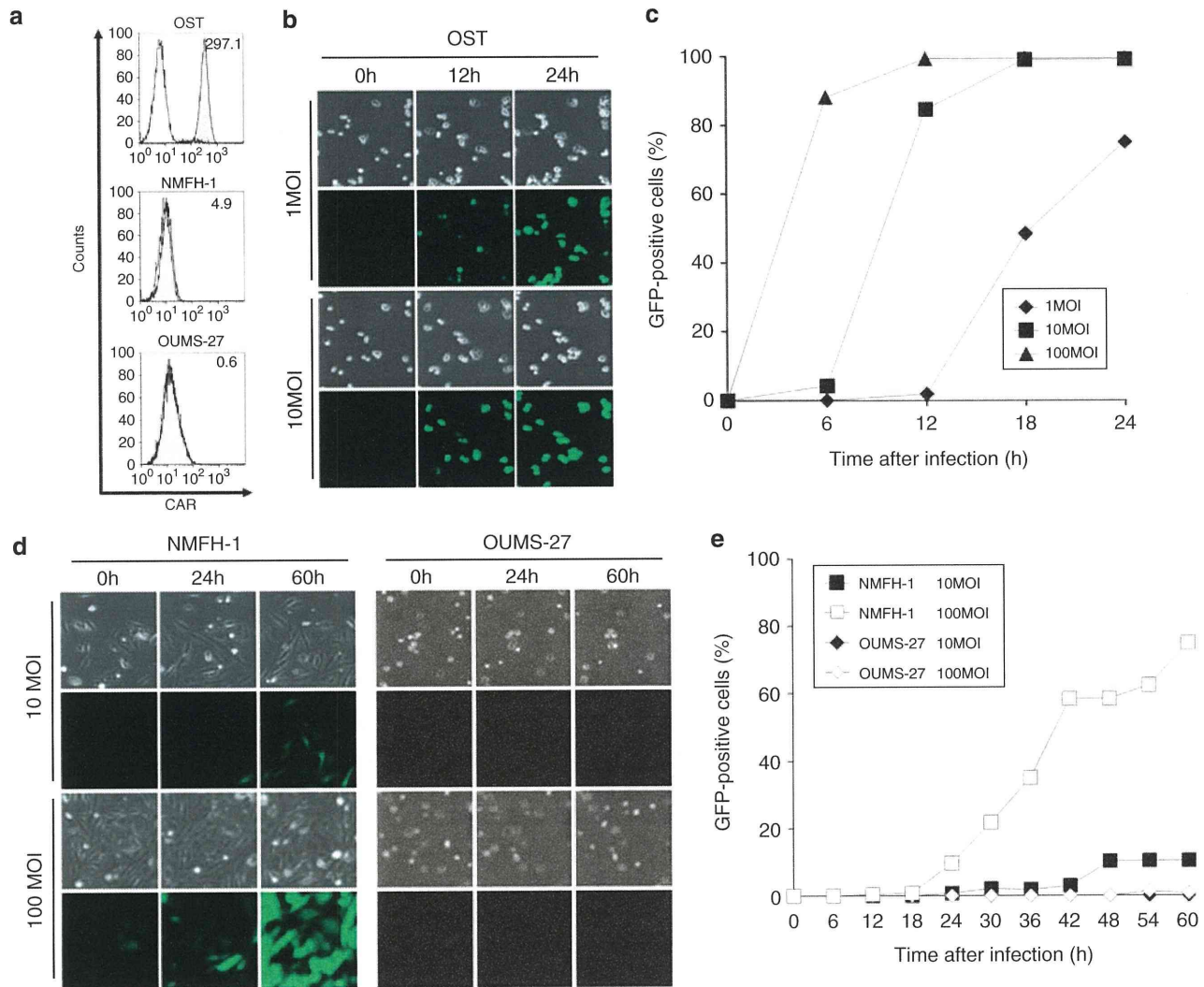
Figure 1. Establishment of a suitable protocol for the detection of CAR expression using OBP-401. (**a**) The level of CAR expression on three human sarcoma cell lines (OST, NMFH-1 and OUMS-27) was analyzed using flow cytometry. The cells were incubated with a monoclonal anti-CAR (RmcB) antibody and the signal was detected using a fluorescent isothiocyanate (FITC)-labeled secondary antibody. The mean fluorescence intensity (MFI), which is a measure of CAR and integrin expression, was calculated for each cell and is shown at the top right of each graph. (**b**) Time-lapse images of OST cells, which displayed the highest CAR expression, were recorded for 24 h after OBP-401 infection at MOIs of 1 and 10 PFU per cell. Representative images taken at the indicated time points and MOIs show cell morphology that was analyzed using phase-contrast microscopy (top panels) and GFP expression that was analyzed using fluorescence microscopy (bottom panels). Original magnification: ×80. (**c**) The percentage of GFP-positive cells was counted in OST cells at the indicated time points after OBP-301 infection at MOIs of 1, 10 and 100 PFU per cell. (**d**) Time-lapse images of non-CAR-expressing OUMS-27 and NMFH-1 cells were recorded for 60 h after OBP-401 infection at MOIs of 10 and 100 PFU per cell. Representative images taken at the indicated time points and MOIs show cell morphology that was analyzed using phase-contrast microscopy (top panels) and GFP expression that was analyzed using fluorescence microscopy (bottom panels). Original magnification: ×80. (**e**) The percentage of OUMS-27 and NMFH-1 GFP-positive cells was counted at the indicated time points after OBP-301 infection at MOIs of 10 and 100 PFU per cell.

mice to develop xenograft tumors. After resection of the OST tumors, the OUMS-27 tumors and normal muscle tissue, the tissues were subjected to the protocol for OBP-401-mediated GFP induction using a three-step procedure (Figure 3a) as follows; step 1: OBP-401 infection for 24 h, step 2: washing with PBS and step 3: observation under a fluorescence microscope. As shown in Figure 3b, OBP-401 infection-induced GFP expression in CAR-positive OST tumor tissues, but not in CAR-negative OUMS-27 tumor tissues or in normal muscle tissue. These results suggest that OBP-401-mediated GFP induction is a simple and useful method for the detection of CAR expression by tumor tissues.

Flow cytometry is a highly sensitive conventional method for the detection of cell surface CAR expression, which is associated with the therapeutic efficacy of Ad5-based vectors in tumor cells.[13,24,28,29] However, as many tumor cells tightly bind to each other or to normal stromal cells within tumor tissues, the preparation of single tumor cells is not easy, and therefore flow cytometry is an inadequate method for the detection of CAR expression in tumor tissues. In contrast, the preparation of single tumor cells is not necessary for the OBP-401-mediated GFP induction protocol. Furthermore, assay of OBP-401-induced GFP expression was more sensitive than flow cytometry (Figure 2d) in distinguishing CAR-positive normal cells from CAR-positive tumor cells (Figure 2c). Thus, the OBP-401-mediated GFP induction method is a simple and tumor-specific system for the detection of CAR expression in tumor tissues.

Fluorescent proteins including GFP have great potentials to visualize tumor cells in real time on the in vivo setting.[37,38]
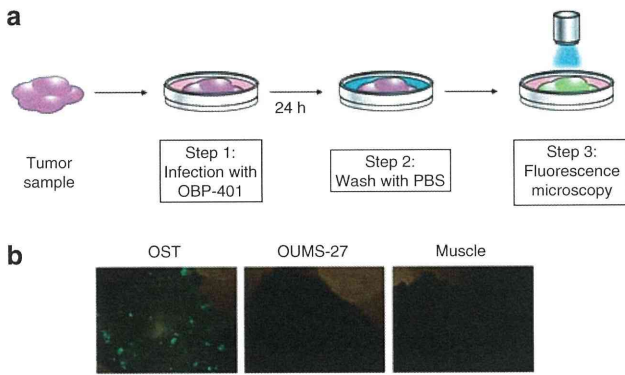
4
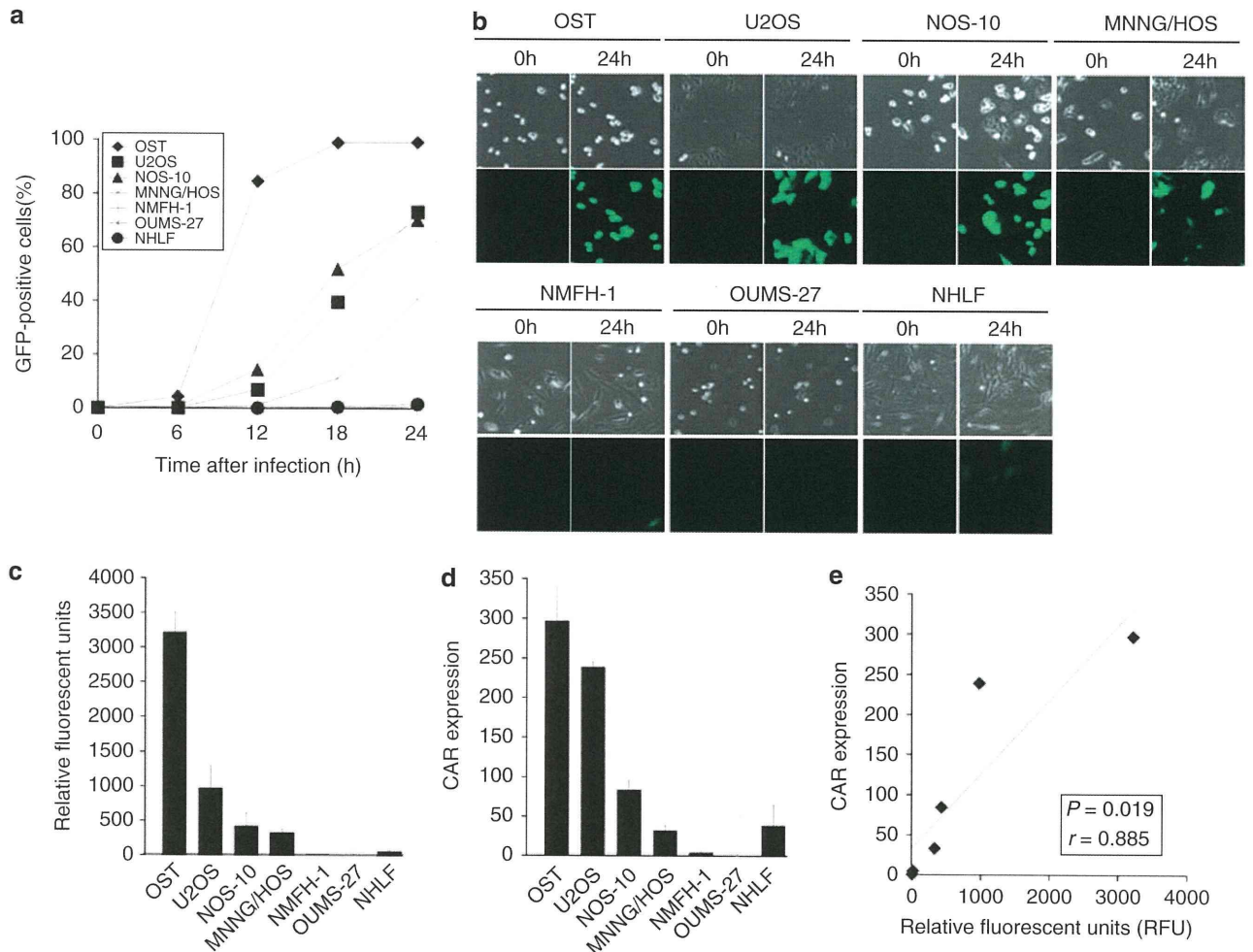
Figure 2. *In vitro* CAR-dependent GFP expression induced by OBP-401 infection. (**a**) The percentage of GFP-positive cells in all tumor and normal cells was counted at the indicated time points after OBP-301 infection at an MOI of 10 PFU per cell. (**b**) Time-lapse images of all tumor and normal cells were recorded for 24 h after infection with OBP-401 at an MOI of 10 PFU per cell. Representative images taken at the indicated time points show cell morphology that was analyzed using phase-contrast microscopy (top panels) and GFP expression that was analyzed using fluorescence microscopy (bottom panels). Original magnification: × 80. (**c**) Quantitative assessment of the level of GFP fluorescence in all tumor and normal cells 24 after OBP-401 infection at an MOI of 10 PFU per cell, using a fluorescent microplate reader with excitation/emission at 485 nm/528 nm. The intensity of GFP fluorescence was evaluated based on the brightness determinations used as relative fluorescent units (RFU). (**d**) The mean fluorescent intensity (MFI) of (CAR) expression on human sarcoma cells and normal fibroblasts. The cells were incubated with a monoclonal anti-CAR (RmcB) antibody, followed by a FITC-labeled secondary antibody, and were analyzed using flow cytometry. (**e**) Relationship between the level of GFP fluorescence and CAR expression in all tumor and normal cells after OBP-401 infection. The slope represents the inverse correlation between these two factors. Statistical significance was determined as $P < 0.05$, after analysis of Pearson's correlation coefficient.

We previously reported that OBP-401 can efficiently induce GFP expression in small populations of metastatic tumor cells at various regions *in vivo*.[32–35] In this study, we further demonstrated that OBP-401-mediated GFP expression provides us the important information for detection of CAR-positive tumor cells. OBP-401 with *hTERT* gene promoter-induced GFP expression in CAR-positive tumor cells with telomerase activity, but not CAR-positive normal cells without telomerase activity (Figure 2c). There was significant relationship between the CAR expression and the GFP expression in tumor cells (Figure 2d). Among the four CAR-positive tumor cells, U2OS cells showed low GFP expression compared with high CAR expression (Figure 1a and 2c). As we recently reported that U2OS cells showed low *hTERT* mRNA expression, the low activity of *hTERT* gene promoter in tumor cells would affect OBP-401-mediated GFP expression. However, as various types of human cancer cells frequently show high telomerase activities,[39] OBP-401-mediated GFP induction system would be widely useful method to evaluate CAR expression in tumor cells.

Previous reports have suggested that *ex vivo* infection of human cancer specimens with a GFP-expressing replication-deficient adenovirus[40] or a replication-selective oncolytic adenovirus[41] is a useful method for assessment of the transduction efficacy or cytopathic activity, respectively, of Ad5-based vectors in individual tumor tissues. In this study, we confirmed that the GFP-expressing telomerase-specific oncolytic adenovirus OBP-401 is useful for detection of CAR-positive tumor tissues through induction of GFP expression (Figure 3b). Interestingly, OBP-401-infected OST tumor tissues showed heterogenous GFP expression (Figure 3b), although GFP expression was induced in all OBP-401-infected OST cells *in vitro* (Figure 2b). Our finding of heterogenous GFP expression in tumor tissues, which indicates heterogenous CAR expression, is consistent with a previously reported heterogeneity in CAR expression.[42] As several factors such as hypoxia[43] and cell cycle status[44] have been suggested to affect CAR expression in tumor cells, factors in the tumor microenvironment may be involved in the heterogenous CAR expression in tumor cells.

47

a

Tumor sample → Step 1: Infection with OBP-401 [24 h] → Step 2: Wash with PBS → Step 3: Fluorescence microscopy

b

OST   OUMS-27   Muscle

Figure 3. A simple method for detection of CAR expression in tumor tissues using OBP-401 infection. (**a**) Outline of the 3-step procedure; step 1: infection with OBP-401, step 2: washing with PBS and step 3: observation under a fluorescence microscope. Tumor tissues ($2 \times 2 \times 2$ mm^3) were infected with OBP-401 at a concentration of 2.4×10^6 PFU for 24 h, were washed with PBS and were observed using fluorescence microscopy. (**b**) Assessment of GFP expression in the CAR-positive OST tumor (left panel), the CAR-negative OUMS-27 tumor (middle panel) and normal muscle tissues (right panel) under a fluorescence microscope. Original magnification: $\times 30$.

Furthermore, as OBP-401 induces tumor-specific GFP expression, normal stromal or epithelial cells may be involved in heterogenous GFP expression in tumor tissues.

In conclusion, we have demonstrated that the GFP-expressing telomerase-specific replication-competent adenovirus OBP-401 is a promising fluorescence imaging tool for the detection of functional and tumor-specific CAR expression in tumor tissues. OBP-401-mediated GFP induction is a simple and highly sensitive method for analysis of tumor cells compared with conventional methods. This novel CAR detection system using OBP-401 has the potential of being widely applicable to assessment of predictive biomarkers for Ad5-based vector-mediated anticancer therapy.

MATERIALS AND METHODS

Cell lines

The human osteosarcoma cell line OST was kindly provided by Dr Satoru Kyo (Kanazawa University, Ishikawa, Japan). The human osteosarcoma cell line U2OS and the transformed embryonic kidney cell line 293 were obtained from the American Type Culture Collection (ATCC; Manassas, VA, USA). The human osteosarcoma cell line NOS-10[45] and the human malignant fibrous histiocytoma cell line NMFH-1[46] were kindly provided by Dr Hiroyuki Kawashima (Niigata University, Niigata, Japan). The human osteosarcoma cell line MNNG/HOS was purchased from DS Pharma Biomedical (Osaka, Japan). The chondrosarcoma cell line OUMS-27 was previously established in our laboratory.[47] The normal human lung fibroblast cell line NHLF was obtained from TaKaRa Biomedicals (Kyoto, Japan). These cells were propagated as monolayer cultures in the medium recommended by the manufacturer. All media were supplemented with 10% heat-inactivated fetal bovine serum, 100 units ml^{-1} penicillin and 100 µg ml^{-1} streptomycin. The cells were maintained at 37 °C in a humidified atmosphere containing 5% CO_2.

Recombinant adenoviruses

We previously generated and characterized OBP-401, which is a telomerase-specific replication-competent adenovirus variant, in which the *hTERT* promoter element drives the expression of *E1A* and *E1B* genes that are linked to an internal ribosome entry site, and in which the *GFP* gene is inserted into the E3 region under a cytomegalovirus promoter.[32,34] The virus was purified by ultracentrifugation using cesium chloride step

gradients. Viral titers were determined by a plaque-forming assay using 293 cells and viruses were stored at -80 °C.

Flow cytometry

The cells (5×10^5 cells) were labeled with the mouse monoclonal anti-CAR (RmcB; Upstate Biotechnology, Lake Placid, NY, USA) antibody for 30 min at 4 °C. The cells were then incubated with fluorescent isothiocyanate-conjugated rabbit anti-mouse IgG second antibody (Zymed Laboratories, San Francisco, CA, USA) and were analyzed using flow cytometry (FACS Array; Becton Dickinson, Mountain View, CA, USA). The mean fluorescence intensity of CAR for each cell line was determined by calculating the differences between the mean fluorescence intensity in antibody-treated and non-treated cells in triplicate experiments.

Time-lapse confocal laser microscopy

The cells (1×10^5 cells per dish) were seeded in 35 mm glass-based dishes 20 h before virus infection. OST cells were infected with OBP-401 at an MOI of 1, 10 or 100 PFU per cell for 24 h. NMFH-1 and OUMS-27 cells were infected with OBP-401 at an MOI of 10 or 100 PFU per cell for 60 h. Other cells were infected with OBP-401 at an MOI of 10 PFU per cell for 24 h. Phase-contrast and fluorescence time-lapse recordings were obtained to concomitantly analyze cell morphology and GFP expression using an inverted FV10i confocal laser scanning microscopy (OLYMPUS; Tokyo, Japan). Photographic images were taken every 5 min. The percentage of GFP-positive cells in each field was calculated using the formula: the number of CAR-positive cells / the total number of CAR-positive and CAR-negative cells $\times 100$.

Fluorescence microplate assay

The cells (5×10^3 cells per well) were seeded on 96-well black bottomed culture plates and were incubated for 20 h before virus infection. The cells were infected with OBP-401 at an MOI of 10 for 24 h. The level of expression of GFP fluorescence was measured using a fluorescent microplate reader (DS Pharma Biomedical; Osaka, Japan) with excitation/emission at 485 nm/528 nm. The mean expression of GFP fluorescence in each cell was calculated in triplicate experiments, as previously reported.[34]

Animal experiments

Animal experimental protocols were approved by the Ethics Review Committee for Animal Experimentation of Okayama University School of Medicine. OST and OUMS-27 cells (5×10^6 cells per site) were inoculated into the flank of female athymic nude mice aged 6 to 7 weeks (Charles River Laboratories, Wilmington, MA, USA). Palpable tumors developed within 14 to 21 days and were permitted to grow to ~ 5 to 6 mm in diameter. At that stage, tumor and normal muscle tissues were resected. The tumor and normal tissues ($2 \times 2 \times 2$ mm^3) were placed in 96-well plates with culture medium. As single tumor cell is about 10 µm in diameter, we considered that there are 2.4×10^5 cells on the surface area of each sample tissue. Then, we infected each sample tissue with 2.4×10^6 PFU (10 MOI per sample) of OBP-401 for 24 h. After washing with PBS, tumor and normal tissues were again placed in 96-well plates with culture medium and analyzed using an inverted fluorescence microscope (OLYMPUS).

Statistical analysis

Data are expressed as means $\pm$ s.d. Student's *t*-test was used to compare differences between groups. Pearson's product-moment correlation coefficients were calculated using PASW statistics software version 18 (SPSS Inc., Chicago, IL, USA). Statistical significance was defined as when the *P* value was less than 0.05.

ABBREVIATIONS

Ad5, Adenovirus serotype 5; CAR, coxsackie and adenovirus receptor; GFP, green fluorescent protein; RT-PCR, reverse transcription-polymerase chain reaction; hTERT, human telomerase reverse transcriptase; MOI, multiplicity of infection;

PFU, plaque-forming unit; IRES, internal ribosome entry site; FITC, fluorescent isothiocyanate; MFI, mean fluorescence intensity.

CONFLICT OF INTEREST

Y Urata is an employee of Oncolys BioPharma, Inc., the manufacturer of OBP-401 (Telomescan). The remaining authors declare no conflict of interest.

REFERENCES

1 Kanerva A, Hemminki A. Adenoviruses for treatment of cancer. *Ann Med* 2005; **37**: 33–43.

2 Rein DT, Breidenbach M, Curiel DT. Current developments in adenovirus-based cancer gene therapy. *Future Oncol* 2006; **2**: 137–143.

3 Yamamoto M, Curiel DT. Current issues and future directions of oncolytic adenoviruses. *Mol Ther* 2010; **18**: 243–250.

4 Clayman GL, el-Naggar AK, Lippman SM, Henderson YC, Frederick M, Merritt JA *et al.* Adenovirus-mediated p53 gene transfer in patients with advanced recurrent head and neck squamous cell carcinoma. *J Clin Oncol* 1998; **16**: 2221–2232.

5 Swisher SG, Roth JA, Nemunaitis J, Lawrence DD, Kemp BL, Carrasco CH *et al.* Adenovirus-mediated p53 gene transfer in advanced non-small-cell lung cancer. *J Natl Cancer Inst* 1999; **91**: 763–771.

6 Shimada H, Matsubara H, Shiratori T, Shimizu T, Miyazaki S, Okazumi S *et al.* Phase I/II adenoviral p53 gene therapy for chemoradiation resistant advanced esophageal squamous cell carcinoma. *Cancer Sci* 2006; **97**: 554–561.

7 Fujiwara T, Tanaka N, Kanazawa S, Ohtani S, Saijo Y, Nukiwa T *et al.* Multicenter phase I study of repeated intratumoral delivery of adenoviral p53 in patients with advanced non-small-cell lung cancer. *J Clin Oncol* 2006; **24**: 1689–1699.

8 Fujiwara T, Urata Y, Tanaka N. Telomerase-specific oncolytic virotherapy for human cancer with the hTERT promoter. *Curr Cancer Drug Targets* 2007; **7**: 191–201.

9 Pesonen S, Kangasniemi L, Hemminki A. Oncolytic adenoviruses for the treatment of human cancer: focus on translational and clinical data. *Mol Pharm* 2011; **8**: 12–28.

10 Bergelson JM, Cunningham JA, Droguett G, Kurt-Jones EA, Krithivas A, Hong JS *et al.* Isolation of a common receptor for Coxsackie B viruses and adenoviruses 2 and 5. *Science* 1997; **275**: 1320–1323.

11 Hemmi S, Geertsen R, Mezzacasa A, Peter I, Dummer R. The presence of human coxsackievirus and adenovirus receptor is associated with efficient adenovirus-mediated transgene expression in human melanoma cell cultures. *Hum Gene Ther* 1998; **9**: 2363–2373.

12 Hutchin ME, Pickles RJ, Yarbrough WG. Efficiency of adenovirus-mediated gene transfer to oropharyngeal epithelial cells correlates with cellular differentiation and human coxsackie and adenovirus receptor expression. *Hum Gene Ther* 2000; **11**: 2365–2375.

13 You Z, Fischer DC, Tong X, Hasenburg A, Aguilar-Cordova E, Kieback DG. Coxsackievirus-adenovirus receptor expression in ovarian cancer cell lines is associated with increased adenovirus transduction efficiency and transgene expression. *Cancer Gene Ther* 2001; **8**: 168–175.

14 Rauen KA, Sudilovsky D, Le JL, Chew KL, Hann B, Weinberg V *et al.* Expression of the coxsackie adenovirus receptor in normal prostate and in primary and metastatic prostate carcinoma: potential relevance to gene therapy. *Cancer Res* 2002; **62**: 3812–3818.

15 Kim M, Zinn KR, Barnett BG, Sumerel LA, Krasnykh V, Curiel DT *et al.* The therapeutic efficacy of adenoviral vectors for cancer gene therapy is limited by a low level of primary adenovirus receptors on tumour cells. *Eur J Cancer* 2002; **38**: 1917–1926.

16 Qin M, Chen S, Yu T, Escuadro B, Sharma S, Batra RK. Coxsackievirus adenovirus receptor expression predicts the efficiency of adenoviral gene transfer into non-small cell lung cancer xenografts. *Clin Cancer Res* 2003; **9**: 4992–4999.

17 Douglas JT, Kim M, Sumerel LA, Carey DE, Curiel DT. Efficient oncolysis by a replicating adenovirus (ad) *in vivo* is critically dependent on tumor expression of primary ad receptors. *Cancer Res* 2001; **61**: 813–817.

18 Fuxe J, Liu L, Malin S, Philipson L, Collins VP, Pettersson RF. Expression of the coxsackie and adenovirus receptor in human astrocytic tumors and xenografts. *Int J Cancer* 2003; **103**: 723–729.

19 Marsee DK, Vadysirisack DD, Morrison CD, Prasad ML, Eng C, Duh QY *et al.* Variable expression of coxsackie-adenovirus receptor in thyroid tumors: implications for adenoviral gene therapy. *Thyroid* 2005; **15**: 977–987.

20 Anders M, Rosch T, Kuster K, Becker I, Hofler H, Stein HJ *et al.* Expression and function of the coxsackie and adenovirus receptor in Barrett's esophagus and associated neoplasia. *Cancer Gene Ther* 2009; **16**: 508–515.

21 Korn WM, Macal M, Christian C, Lacher MD, McMillan A, Rauen KA *et al.* Expression of the coxsackievirus- and adenovirus receptor in gastrointestinal cancer correlates with tumor differentiation. *Cancer Gene Ther* 2006; **13**: 792–797.

22 Gu W, Ogose A, Kawashima H, Ito M, Ito T, Matsuba A *et al.* High-level expression of the coxsackievirus and adenovirus receptor messenger RNA in osteosarcoma, Ewing's sarcoma, and benign neurogenic tumors among musculoskeletal tumors. *Clin Cancer Res* 2004; **10**: 3831–3838.

23 Kawashima H, Ogose A, Yoshizawa T, Kuwano R, Hotta Y, Hotta T *et al.* Expression of the coxsackievirus and adenovirus receptor in musculoskeletal tumors and mesenchymal tissues: efficacy of adenoviral gene therapy for osteosarcoma. *Cancer Sci* 2003; **94**: 70–75.

24 Rice AM, Currier MA, Adams LC, Bharatan NS, Collins MH, Snyder JD *et al.* Ewing sarcoma family of tumors express adenovirus receptors and are susceptible to adenovirus-mediated oncolysis. *J Pediatr Hematol Oncol* 2002; **24**: 527–533.

25 Matsumoto K, Shariat SF, Ayala GE, Rauen KA, Lerner SP. Loss of coxsackie and adenovirus receptor expression is associated with features of aggressive bladder cancer. *Urology* 2005; **66**: 441–446.

26 Anders M, Vieth M, Rocken C, Ebert M, Pross M, Gretschel S *et al.* Loss of the coxsackie and adenovirus receptor contributes to gastric cancer progression. *Br J Cancer* 2009; **100**: 352–359.

27 Yamamoto S, Yoshida Y, Aoyagi M, Ohno K, Hirakawa K, Hamada H. Reduced transduction efficiency of adenoviral vectors expressing human p53 gene by repeated transduction into glioma cells *in vitro*. *Clin Cancer Res* 2002; **8**: 913–921.

28 Tango Y, Taki M, Shirakiya Y, Ohtani S, Tokunaga N, Tsunemitsu Y *et al.* Late resistance to adenoviral p53-mediated apoptosis caused by decreased expression of Coxsackie-adenovirus receptors in human lung cancer cells. *Cancer Sci* 2004; **95**: 459–463.

29 Sasaki T, Tazawa H, Hasei J, Kunisada T, Yoshida A, Hashimoto Y *et al.* Preclinical evaluation of telomerase-specific oncolytic virotherapy for human bone and soft tissue sarcomas. *Clin Cancer Res* 2011; **17**: 1828–1838.

30 Kawashima T, Kagawa S, Kobayashi N, Shirakiya Y, Umeoka T, Teraishi F *et al.* Telomerase-specific replication-selective virotherapy for human cancer. *Clin Cancer Res* 2004; **10** (1 Pt 1): 285–292.

31 Hashimoto Y, Watanabe Y, Shirakiya Y, Uno F, Kagawa S, Kawamura H *et al.* Establishment of biological and pharmacokinetic assays of telomerase-specific replication-selective adenovirus. *Cancer Sci* 2008; **99**: 385–390.

32 Kishimoto H, Kojima T, Watanabe Y, Kagawa S, Fujiwara T, Uno F *et al.* In vivo imaging of lymph node metastasis with telomerase-specific replication-selective adenovirus. *Nat Med* 2006; **12**: 1213–1219.

33 Kishimoto H, Urata Y, Tanaka N, Fujiwara T, Hoffman RM. Selective metastatic tumor labeling with green fluorescent protein and killing by systemic administration of telomerase-dependent adenoviruses. *Mol Cancer Ther* 2009; **8**: 3001–3008.

34 Kojima T, Hashimoto Y, Watanabe Y, Kagawa S, Uno F, Kuroda S *et al.* A simple biological imaging system for detecting viable human circulating tumor cells. *J Clin Invest* 2009; **119**: 3172–3181.

35 Kishimoto H, Zhao M, Hayashi K, Urata Y, Tanaka N, Fujiwara T *et al.* In vivo internal tumor illumination by telomerase-dependent adenoviral GFP for precise surgical navigation. *Proc Natl Acad Sci USA* 2009; **106**: 14514–14517.

36 Feero WG, Rosenblatt JD, Huard J, Watkins SC, Epperly M, Clemens PR *et al.* Viral gene delivery to skeletal muscle: insights on maturation-dependent loss of fiber infectivity for adenovirus and herpes simplex type 1 viral vectors. *Hum Gene Ther* 1997; **8**: 371–380.

37 Hoffman RM. The multiple uses of fluorescent proteins to visualize cancer *in vivo*. *Nat Rev Cancer* 2005; **5**: 796–806.

38 Hoffman RM, Yang M. Subcellular imaging in the live mouse. *Nat Protoc* 2006; **1**: 775–782.

39 Shay JW, Bacchetti S. A survey of telomerase activity in human cancer. *Eur J Cancer* 1997; **33**: 787–791.

40 Marsman WA, Buskens CJ, Wesseling JG, Offerhaus GJ, Bergman JJ, Tytgat GN *et al.* Gene therapy for esophageal carcinoma: the use of an explant model to test adenoviral vectors *ex vivo*. *Cancer Gene Ther* 2004; **11**: 289–296.

41 Wang Y, Thorne S, Hannock J, Francis J, Au T, Reid T *et al.* A novel assay to assess primary human cancer infectibility by replication-selective oncolytic adenoviruses. *Clin Cancer Res* 2005; **11**: 351–360.

42 Zeimet AG, Muller-Holzner E, Schuler A, Hartung G, Berger J, Hermann M *et al.* Determination of molecules regulating gene delivery using adenoviral vectors in ovarian carcinomas. *Gene Therapy* 2002; **9**: 1093–1100.

43 Kuster K, Koschel A, Rohwer N, Fischer A, Wiedenmann B, Anders M. Downregulation of the coxsackie and adenovirus receptor in cancer cells by hypoxia depends on HIF-1alpha. *Cancer Gene Ther* 2010; **17**: 141–146.

44 Seidman MA, Hogan SM, Wendland RL, Worgall S, Crystal RG, Leopold PL. Variation in adenovirus receptor expression and adenovirus vector-mediated transgene expression at defined stages of the cell cycle. *Mol Ther* 2001; **4**: 13–21.

45 Hotta T, Motoyama T, Watanabe H. Three human osteosarcoma cell lines exhibiting different phenotypic expressions. *Acta Pathol Jpn* 1992; **42**: 595–603.

46 Kawashima H, Ogose A, Gu W, Nishio J, Kudo N, Kondo N *et al.* Establishment and characterization of a novel myxofibrosarcoma cell line. *Cancer Genet Cytogenet* 2005; **161**: 28–35.

47 Kunisada T, Miyazaki M, Mihara K, Gao C, Kawai A, Inoue H *et al.* A new human chondrosarcoma cell line (OUMS-27) that maintains chondrocytic differentiation. *Int J Cancer* 1998; **77**: 854–859.

Supplementary Information accompanies the paper on Gene Therapy website (http://www.nature.com/gt)

A novel apoptotic mechanism of genetically engineered adenovirus-mediated tumour-specific p53 overexpression through E1A-dependent p21 and MDM2 suppression

Yasumoto Yamasaki [a], Hiroshi Tazawa [a,b], Yuuri Hashimoto [a], Toru Kojima [a], Shinji Kuroda [a], Shuya Yano [a], Ryosuke Yoshida [a], Futoshi Uno [a], Hiroyuki Mizuguchi [c], Akira Ohtsuru [d], Yasuo Urata [e], Shunsuke Kagawa [a], Toshiyoshi Fujiwara [a,*]

[a] *Department of Gastroenterological Surgery, Okayama University Graduate School of Medicine, Dentistry and Pharmaceutical Sciences, Okayama 700-8558, Japan*
[b] *Center for Gene and Cell Therapy, Okayama University Hospital, Okayama 700-8558, Japan*
[c] *Department of Biochemistry and Molecular Biology, Graduate School of Pharmaceutical Sciences, Osaka University, Osaka 565-0871, Japan*
[d] *Takashi Nagai Memorial International Hibakusha Medical Center, Nagasaki University Hospital, Nagasaki 852-8501, Japan*
[e] *Oncolys BioPharma Inc., Tokyo 105-0001, Japan*

KEYWORDS
Oncolytic adenovirus
Telomerase
p53
Apoptosis
p21

Abstract Oncolytic viruses engineered to replicate in tumour cells but not in normal cells could be used as tumour-specific vectors carrying the therapeutic genes. We previously developed a telomerase-specific oncolytic adenovirus, OBP-301, that causes cell death in human cancer cells with telomerase activities. Here, we further modified OBP-301 to express the wild-type *p53* tumour suppressor gene (OBP-702), and investigated whether OBP-702 induces stronger antitumour activity than OBP-301. The antitumour effect of OBP-702 was compared to that of OBP-301 on OBP-301-sensitive (H358 and H460) and OBP-301-resistant (T.Tn and HSC4) human cancer cells. OBP-702 suppressed the viability of both OBP-301-sensitive and OBP-301-resistant cancer cells more efficiently than OBP-301. OBP-702 caused increased apoptosis compared to OBP-301 or a replication-deficient adenovirus expressing the *p53* gene (Ad-p53) in H358 and T.Tn cells. Adenovirus E1A-mediated p21 and MDM2 downregulation was involved in the apoptosis caused by OBP-702. Moreover, OBP-702 significantly suppressed tumour growth in subcutaneous tumour xenograft models compared to monotherapy with OBP-301 or Ad-p53. Our data demonstrated that OBP-702 infection expressed adenovirus E1A and then inhibited p21 and MDM2 expression, which in turn efficiently induced apoptotic cell death. This novel apoptotic mechanism suggests that the p53-expressing OBP-702 is a promising antitumour reagent for human cancer and could improve the clinical outcome.
© 2011 Elsevier Ltd. All rights reserved.

* *Corresponding author:* Address: Department of Gastroenterological Surgery, Okayama University Graduate School of Medicine, Dentistry and Pharmaceutical Sciences, 2-5-1 Shikata-cho, Kita-ku, Okayama 700-8558, Japan. Tel.: +81 86 235 7257; fax: +81 86 221 8775.
  E-mail address: toshi_f@md.okayama-u.ac.jp (T. Fujiwara).

1. Introduction

Replication-selective oncolytic viruses have emerged as promising antitumour reagents for induction of tumour-specific cell death.[1–4] Recent evidence from several clinical studies of oncolytic virotherapy has suggested that oncolytic viruses are well tolerated by cancer patients.[5–8] We previously developed a telomerase-specific replication-competent oncolytic adenovirus OBP-301 (Telomelysin), in which the human telomerase reverse transcriptase (*hTERT*) promoter drives the expression of the *E1A* and *E1B* genes that are linked to an internal ribosome entry site (IRES).[9–11] A phase I clinical trial of OBP-301 in patients with advanced solid tumours has been recently completed and OBP-301 was well tolerated by these patients.[12] However, the antitumour effect of OBP-301 was limited in some of the OBP-301-injected tumours. Therefore, to efficiently eliminate tumour cells using OBP-301, and to improve the clinical outcome of cancer patients, enhancement of the OBP-301-mediated antitumour effect is required.

Genetically engineered armed oncolytic viruses that express several types of therapeutic transgenes have recently been reported that were aimed at enhancing the antitumour effect of an oncolytic virus.[6,13] Among candidate therapeutic transgenes, the tumour-suppressor *p53* gene is a potent therapeutic transgene for induction of cell cycle arrest, senescence and apoptosis.[14] Indeed, a p53-expressing replication-deficient adenovirus (Ad-p53, Advexin) has been reported to induce an antitumour effect in both *in vitro* and *in vivo* settings[15,16] as well as in various clinical studies.[17–20] Recently, p53-expressing armed replication-selective oncolytic adenoviruses have been shown to induce a stronger antitumour effect than a non-armed oncolytic adenovirus or Ad-p53.[21–23] However, the molecular mechanism of the enhanced antitumour effect of a p53-armed oncolytic adenovirus remains unclear. We recently showed that, in combination therapy, OBP-301 enhanced Ad-p53-mediated apoptosis through p53 upregulation and by suppression of the p53-downstream target p21,[24] which is not only transcriptionally activated and mainly induces cell cycle arrest, but also suppresses apoptosis.[25] These results suggest that this p53-expressing oncolytic adenovirus has a strong antitumour effect through apoptosis induction.

In the present study, we first investigated whether the p53-expressing telomerase-specific replication-competent oncolytic adenovirus OBP-702 has efficient *in vitro* antitumour activity compared with OBP-301. We next compared the induction of apoptotic cell death of human cancer cells infected with OBP-301, OBP-702 and Ad-p53. The molecular mechanism of OBP-702-mediated apoptosis induction was further addressed. Finally, the *in vivo* antitumour effect of OBP-702 was evaluated using two subcutaneous human tumour xenograft models.

2. Materials and methods

2.1. Cell lines

The human non-small cell lung cancer cell lines H1299 (p53 null), H358 (p53 null) and H460 (wild-type p53) were obtained from the American Type Culture Collection (Manassas, VA, USA). The human oesophageal cancer cell line T.Tn (mutant-type p53) was purchased from the Japanese Collection Research Bioresources (JCRB, Osaka, Japan). The human oral squamous cell carcinoma cell line HSC4 (wild-type p53) was obtained from the Human Science Research Resources Bank (HSRRB, Osaka, Japan). The human colon cancer cell lines (SW620 (mutant-type p53) and LoVo (wild-type p53)) and the human liver cancer cell line HepG2 (wild-type p53) were obtained from the American Type Culture Collection (Manassas, VA, USA). The human liver cancer cell line Huh-7 (mutant-type p53) was obtained from the Human Science Research Resources Bank (HSRRB, Osaka, Japan). H1299, H358, H460, T.Tn, SW620 and LoVo cells were maintained in RPMI 1640 medium. HSC4, HepG2 and Huh-7 cells were maintained in Dulbecco's modified Eagle's medium. All media were supplemented with 10% foetal bovine serum, 100 U/ml penicillin and 100 mg/ml streptomycin. The cells were routinely maintained at 37 °C in a humidified atmosphere containing 5% CO_2.

2.2. Recombinant adenoviruses

The recombinant telomerase-specific, replication-competent adenovirus OBP-301 (Telomelysin), in which the promoter element of the *hTERT* gene drives the expression of *E1A* and *E1B* genes that are linked with an IRES, was previously constructed and characterised.[9–11] For OBP-301 induction of exogenous *p53* gene expression, a human wild-type *p53* gene expression cassette derived by the Egr-1 promoter was inserted into the E3 region of OBP-301 (Fig. 1A). The E1A-deleted adenoviral vector dl312 and the wild-type adenovirus type 5 (Ad5) were used as control vectors. Recombinant viruses were purified by ultracentrifugation using caesium chloride step gradients, their titres were determined by a plaque-forming assay using 293 cells, and viruses were stored at −80 °C.

2.3. Western blot analysis

Cells were seeded in a 100-mm dish at a density of 1×10^5 cells/dish 12 h before infection and were infected with OBP-301, OBP-702 or Ad-p53 at the indicated multiplicity of infection (MOI). Whole cell lysates were prepared in a lysis buffer (50 mM Tris–HCl (pH 7.4), 150 mM NaCl, 1% Triton X-100) containing a protease inhibitor cocktail (Complete Mini; Roche, Indianapolis,

IN, USA) at the indicated time points. Proteins were electrophoresed on 6–15% SDS polyacrylamide gels and were transferred to polyvinylidene difluoride membranes (Hybond-P; GE Healthcare, Buckinghamshire, UK). Blots were blocked with 5% non-fat dry milk in TBS-T (Tris-buffered saline and 0.1% Tween-20, pH 7.4) at room temperature for 30 min. The primary antibodies used were: mouse anti-p53 monoclonal antibody (mAb) (Calbiochem, Darmstadt, Germany), mouse anti-p21[WAF1] mAb (Calbiochem), mouse anti-MDM2 mAb (Santa Cruz Biotechnology, Santa Cruz, CA, USA), rabbit anti-BAX polyclonal antibody (pAb) (Santa Cruz Biotechnology), rabbit anti-poly (ADP-ribose) polymerase (PARP) pAb (Cell Signaling Technology, Beverly, MA, USA), mouse anti-Ad5 E1A mAb (BD PharMingen, Franklin Lakes, NJ, USA) and mouse anti-β-actin mAb (Sigma–Aldrich, St. Louis, MO, USA). The secondary antibodies used were: horseradish peroxidase-conjugated antibodies against rabbit IgG (GE Healthcare) or mouse IgG (GE Healthcare). Immunoreactive bands on the blots were visualised using enhanced chemiluminescence substrates (ECL Plus; GE Healthcare).

2.4. Cell viability assay

Cells were seeded on 96-well plates at a density of 1×10^3 cells/well 12 h before infection and were infected with OBP-301 or OBP-702 at MOIs of 0, 0.1, 1, 10 or 100 plaque-forming units (PFU)/cell. Cell viability was determined on days 2, 3 and 5 after virus infection using the Cell Proliferation Kit II (Roche Molecular Biochemicals, Indianapolis, IN, USA), which is based on an XTT, sodium 3′-[1-(phenylaminocarbonyl)-3,4-tetrazolium]-bis(4-methoxy-6-nitro)benzene sulphonic acid hydrate assay, according to the manufacturer's protocol. The 50% inhibiting dose (ID_{50}) value of OBP-301 and OBP-702 for each cell line was calculated using cell viability data obtained on day 5 after virus infection.

2.5. Flow cytometric analysis of active caspase-3 expression

Cells were incubated for 20 min on ice in Cytofix/Cytoperm solution (BD Biosciences, Franklin Lakes, NJ, USA), were labelled with phycoerythrin-conjugated rabbit anti-active caspase-3 mAb (BD Biosciences) for
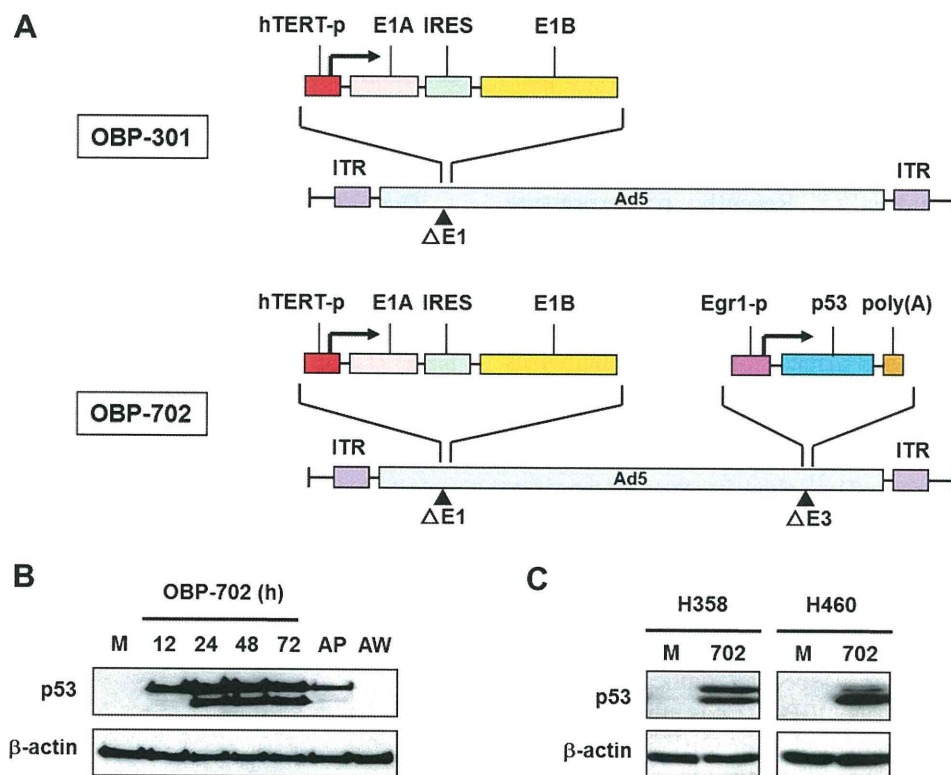

Fig. 1. p53 upregulation in human cancer cells infected with OBP-702. (A) Schematic diagrams of OBP-301 and OBP-702 structures. OBP-301 is a telomerase-specific replication-competent adenovirus, in which the *hTERT* promoter drives the expression of *E1A* and *E1B* genes that are linked with an IRES. OBP-702 is a p53-armed OBP-301, in which the *Egr-1* promoter drives expression of the *p53* gene that is inserted into the E3 region. (B) Expression of the p53 protein in p53-null H1299 cells infected with OBP-702 (10 MOI) at the indicated time points. A replication-deficient p53-expressing adenovirus Ad-p53 (AP) and a wild-type adenovirus Ad5 (AW) were also infected at an MOI of 10 for 24 h as a positive and negative control, respectively. Cell lysates were subjected to Western blot analysis with an anti-p53 antibody. β-Actin was assayed as a loading control. (C) Expression of the p53 protein in H358 and H460 cells infected with OBP-702 (702) at an MOI of 10 for 24 h. Mock-infected cells (M) were used as controls.

30 min, and were then analysed using FACS array (BD Biosciences).

2.6. In vivo subcutaneous H358 and T.Tn xenograft tumour models

Animal experimental protocols were approved by the Ethics Review Committee for Animal Experimentation of Okayama University School of Medicine. The H358 and T.Tn cells (5×10^6 cells per site) were inoculated into the flanks of 5-week-old female athymic nude mice (Charles River Laboratories, Wilmington, MA, USA). When tumours reached approximately 5–6 mm in diameter, a 50 μl volume of solution containing OBP-301, OBP-702 or Ad-p53 at a dose of 1×10^8 PFU or phosphate buffered saline (PBS) was injected into the tumours for three cycles every 2 days. Tumour size was monitored by measuring tumour length and width using calipers. Each tumour volume was calculated using the following formula: tumour volume $(mm^3) = L \times W^2 \times 0.5$, where L is the length and W is the width. The survival rate of mice with H358 tumours or T.Tn tumours was assessed until 90 or 180 days, respectively, after first treatment.

2.7. Statistical analysis

Data are expressed as means ± standard deviation (SD). Student's t test was used to compare differences between groups. Log-rank test was also used to compare differences between groups in the survival rate of mice. Statistical significance was defined as a P value less than 0.05.

3. Results

3.1. p53 induction in human cancer cells infected with OBP-702

To examine the level of p53 expression induced by OBP-702 in human cancer cells, we first evaluated p53 expression of p53-null human lung cancer H1299 cells after OBP-702 infection using Western blot analysis. The p53 expression level was increased within 24 h after OBP-702 infection, and a high expression level was maintained for up to 72 h (Fig. 1B). OBP-702-induced p53 expression was higher than Ad-p53-induced p53 expression 24 h after infection. Detectable 40 kDa protein expression in OBP-702-infected H1299 cells may be due to higher p53 expression. In contrast, no p53 expression was induced by OBP-301 infection (data not shown). OBP-702 further induced p53 expression in other human lung cancer cells (H358 (p53-null) and H460 (wild-type p53)) and in human colon cancer cells (SW620 (mutant p53), LoVo cells (wild-type p53)) and human liver cancer cells (HepG2 (wild-type p53) and Huh7 (mutant p53)) (Fig. 1C and Supplementary

Fig. 1A). These results indicate that OBP-702 efficiently induces exogenous p53 expression in human cancer cells independent of the status of endogenous p53.

3.2. OBP-702 has enhanced antitumour activity against human cancer cells compared to OBP-301

To compare the *in vitro* antitumour activity of OBP-702 and OBP-301, we used the two OBP-301-sensitive human cancer cells (H358 and H460) and the two OBP-301-resistant human cancer cells (T.Tn and HSC4) that were previously reported.[11] OBP-301-resistant cells showed lower the coxsackie and adenovirus receptor (CAR) expression compared to OBP-301-sensitive cells (data not shown). The cell viability of each cell line was assessed over 5 days after infection using the XTT assay. OBP-702 suppressed the viability of OBP-301-sensitive and OBP-301-resistant cells more efficiently than OBP-301, although at least 48 h are required for the sufficient viral replication (Fig. 2A). Furthermore, OBP-702 also showed increased antitumour activity against human colon and liver cancer cells compared to OBP-301 (Supplementary Fig. 1B). Calculation of the ID_{50} values indicated that all cell lines were more sensitive to OBP-702 than to OBP-301 (Supplementary Table S1). These results suggest that OBP-702 is more cytopathic for human cancer cells than OBP-301.

3.3. Increased induction of apoptosis by OBP-702 compared to OBP-301 or Ad-p53

We next investigated whether OBP-702 has a greater apoptotic effect than OBP-301 or Ad-p53. OBP-301-sensitive H358 cells and OBP-301-resistant T.Tn cells were each infected with OBP-702, OBP-301 or Ad-p53 at MOIs of 10 and 100 for 48 h, and apoptosis was analysed. Western blot analysis showed that OBP-702, but not OBP-301 or Ad-p53, induced the cleavage of PARP at 48 and 72 h after infection (Fig. 3A). Furthermore, flow cytometric analysis demonstrated that OBP-702 infection significantly increased the percentage of apoptotic H358 and T.Tn cells that expressed active caspase-3 compared to Ad-p53 infection (Fig. 3B and C). However, no apoptosis was induced after OBP-301 infection. These results suggest that OBP-702 has a stronger effect on apoptosis than Ad-p53 or OBP-301.

3.4. Induction of apoptosis by OBP-702 through p53-dependent BAX upregulation and E1A-dependent p21 and MDM2 downregulation

Overexpression of p53 is well known to induce apoptosis through induction of p53-downstream target genes.[14] To investigate the molecular mechanism of OBP-702-induced apoptotic cell death, the expression
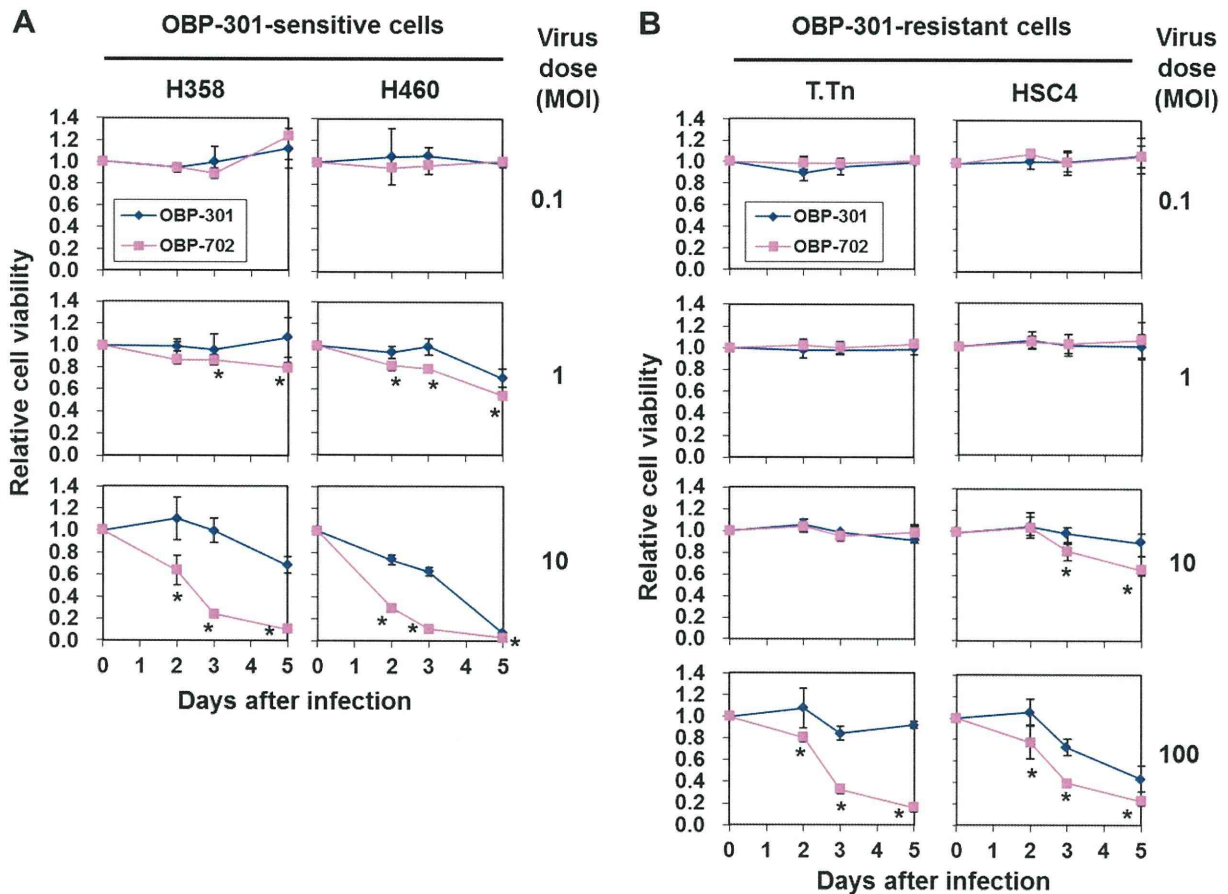
Fig. 2. OBP-702 has enhanced antitumour activity against human cancer cells compared to OBP-301. OBP-301-sensitive cells (H358 and H460) (A) and OBP-301-resistant cells (T.Tn and HSC4) (B) were infected with OBP-301 or OBP-702 at the indicated doses and cell viability was measured using the XTT assay on days 2, 3 and 5 after infection. Cell viability was calculated relative to that of the mock-treated group on each day, which was set at 1.0. Cell viability data are expressed as mean values ± SD ($n = 5$). Statistical significance was determined using Student's t test. $^{*}P < 0.05$. The data are representative of three separate experiments.

level of p53, and p53-downstream target proteins such as p21, BAX and MDM2, was evaluated by Western blot analysis. OBP-702 infection induced higher p53 expression than that induced by Ad-p53 between 24 and 72 h after infection (Fig. 4A). Ad-p53 infection upregulated the expression of p21, MDM2 and BAX proteins. In contrast, OBP-702 infection upregulated the BAX protein as well as Ad-p53, but expression of p21 and MDM2 was low despite strong p53 activation. PARP cleavage was observed 48 and 72 h after OBP-702 infection, consistent with suppression of p21 and MDM2 expression. Overexpression of the adenoviral E1A protein was observed in OBP-702-infected cells. These results suggest that OBP-702 upregulates p53 expression and subsequent BAX expression, but downregulates p21 and MDM2 expression, resulting in the induction of apoptosis.

We recently reported that OBP-301 enhances Ad-p53-induced apoptosis through p53 overexpression and p21 suppression.[24] Furthermore, adenovirus-mediated E2F1 overexpression also enhanced Ad-p53-induced apoptosis through MDM2 downregulation.[26] Since

adenoviral E1A is known to activate E2F1 expression,[27] we hypothesised that OBP-702-mediated E1A expression may enhance Ad-p53-induced apoptosis through suppression of p21 and MDM2 expression. To address this hypothesis, H358 cells were coinfected with E1A-deficient dl312 or E1A-expressing wild-type Ad5 after Ad-p53 infection. Ad-p53-induced p53 overexpression was enhanced in the Ad5-coinfected H358 cells, but not in the dl312-coinfected H358 cells (Fig. 4B). Consistent with p53 overexpression, BAX expression was also upregulated. However, despite the enhanced p53 expression, the expression of p21 and MDM2 proteins was lower in Ad5-coinfected cells than in dl312-coinfected cells. Furthermore, PARP cleavage was only detected in H358 cells 72 h after coinfection of Ad-p53 with Ad5. As expected, OBP-301 infection had no apparent effect of the expression of p53, and p53-downstream target proteins (Supplementary Fig. 2). These results suggest that adenoviral E1A suppresses the expression of p21 and MDM2 thereby enhancing apoptosis through p53-dependent BAX upregulation (Fig. 4C, Supplementary Fig. 3).
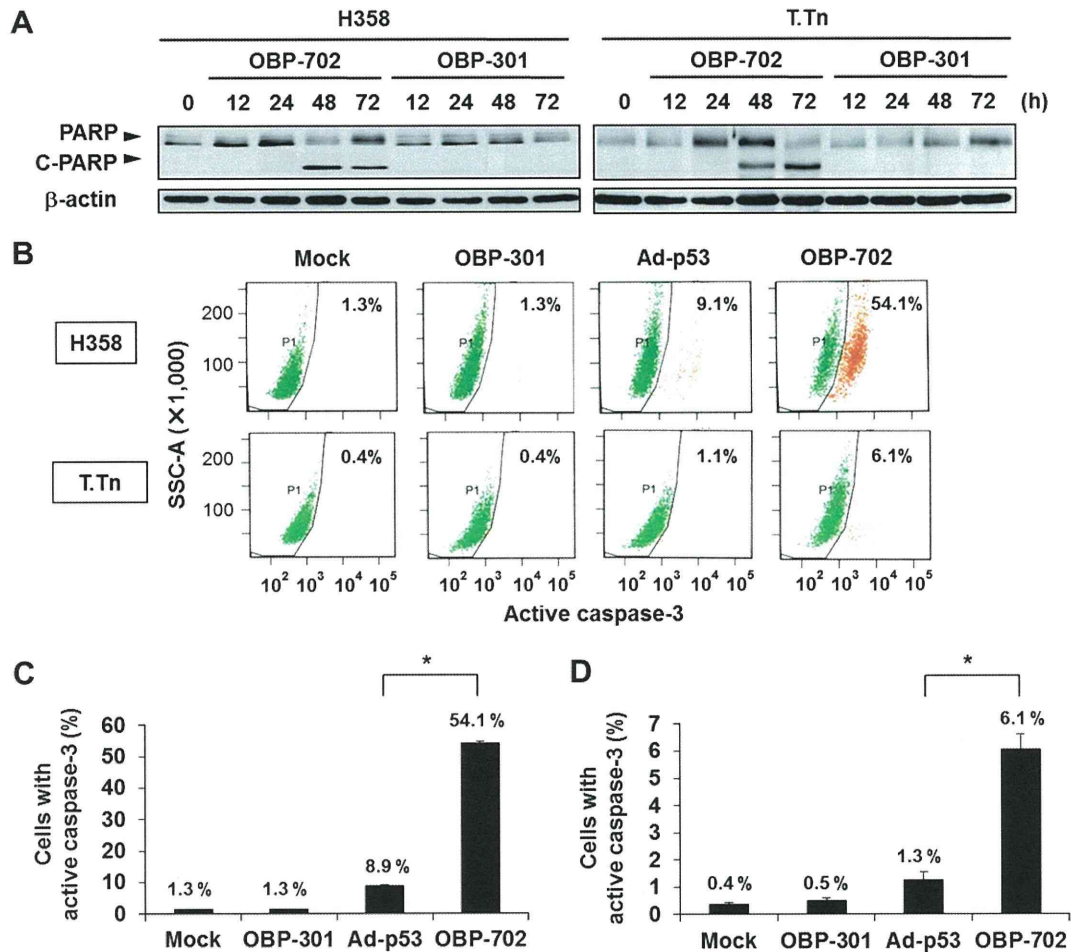
Fig. 3. OBP-702 induces increased apoptosis compared to OBP-301 or Ad-p53. (A) OBP-301-sensitive H358 cells and OBP-301-resistant T.Tn cells were infected with OBP-301 or OBP-702 at an MOI of 10 and 100, respectively, for 48 h. The level of cleaved PARP (C-PARP) and intact PARP in cell lysates was analysed using Western blotting. β-Actin was assayed as a loading control. (B–D), H358 and T.Tn cells were infected with OBP-702, OBP-301 or Ad-p53 at an MOI of 10 and 100, respectively, for 48 h. Mock-infected cells were used as controls. Caspase-3 activation was quantified using flow cytometric analysis. Representative flow cytometric data are shown (B). The mean percentage of H358 cells (C) and T.Tn cells (D) that express active caspase-3 was calculated based on three-independent experiments. Bars, SD. Statistical significance was determined using Student's *t* test. $^{*}P < 0.05$.

3.5. Enhanced antitumour effect of OBP-702 in tumour xenograft animal models

Finally, to assess the *in vivo* antitumour effect of OBP-702, we used subcutaneous H358 and T.Tn tumour xenograft models. OBP-702, OBP-301, Ad-p53 or PBS was intratumourally injected for three cycles every 2 days. OBP-702 administration significantly suppressed tumour growth compared to OBP-301, Ad-p53 or PBS in H358 and T.Tn tumour xenograft models (Fig. 5A). Furthermore, H358 tumour-bearing mice treated with OBP-702 significantly survived longer than those treated with OBP-301 or Ad-p53 (Fig. 5B). Although there was no significant difference in the survival rates between OBP-702-treated and OBP-301-treated mice with T.Tn tumours, OBP-702 treatment significantly increased the survival rate of T.Tn tumour-bearing mice compared to Ad-p53. These results suggest that OBP-702 eliminates tumour tissues more efficiently than OBP-301 or Ad-p53.

4. Discussion

Genetically engineered transgene-expressing armed oncolytic adenoviruses are expected to be a third-generation oncolytic virus for induction of a strong antitumour effect through induction of oncolytic and transgene-induced cell death.[6,13] Although the tumour suppressor *p53* gene is a potent therapeutic transgene for enhancement of an oncolytic adenovirus-mediated antitumour effect,[21–23] the molecular mechanisms by which p53 mediates enhancement of the antitumour effect remain unclear. In this study, we showed that the p53-expressing telomerase-specific oncolytic adenovirus OBP-702 exerted stronger *in vitro* and *in vivo* antitumour effects than OBP-301 or Ad-p53 (Figs. 2 and 5). This enhanced antitumour effect was due to p53-induced apoptosis, and adenoviral E1A enhanced this apoptosis via suppression of the expression of anti-apoptotic p21 and p53-inhibitory MDM2 (Figs. 3 and 4). Although
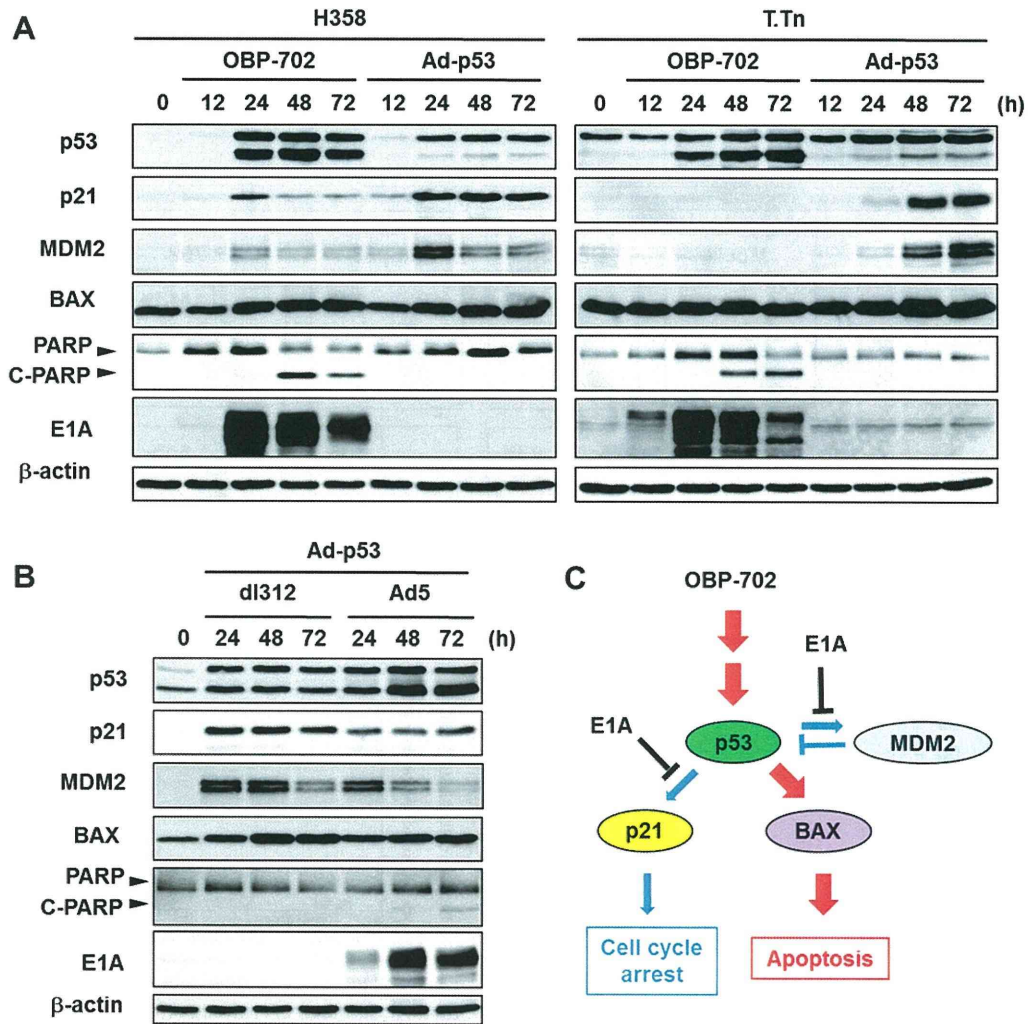
Fig. 4. OBP-702-mediated activation of p53, p53-target proteins and PARP in an E1A-dependent manner. (A) H358 and T.Tn cells were infected with OBP-702 or Ad-p53 at an MOI of 10 and 100, respectively, and infected cells were harvested at the indicated time points. The level of p53, p21, MDM2, BAX, PARP, cleaved PARP (C-PARP) and E1A proteins in cell lysates was analysed by Western blotting. β-Actin was assayed as a loading control. (B) H358 cells were infected with Ad-p53, following which they were coinfected with the E1A-deficient adenovirus (dl312) or an E1A-expressing wild-type adenovirus (Ad5) at the indicated time points. (C) Outline of OBP-702-mediated apoptosis induction through p53-dependent BAX upregulation and E1A-dependent downregulation of p21 and MDM2.

replication-competent adenovirus-mediated *p53* gene transduction has been suggested to exert an increased antitumour effect compared to replication-deficient Ad-p53 through replication-mediated p53 overexpression,[22] adenoviral E1A also enhanced p53-mediated apoptosis through suppression of expression of the p53-downstream targets p21 and MDM2 (Fig. 4). The adenoviral E1A protein has been previously shown to suppress p53-induced p21 and MDM2 expression.[28,29] E1A-mediated p21 and MDM2 suppression has also been shown to induce apoptosis in DNA-damaged cells that overexpress p53.[30,31] These reports support our findings that adenoviral E1A protein enhances p53-induced apoptosis through p21 and MDM2 suppression. It has recently been further shown that replication-deficient Ad-p53 enhances apoptosis through p21 suppression in combination with artificial microRNAs[32] or with OBP-301.[24] Thus, replication-competent

oncolytic adenovirus-mediated *p53* gene transfer would strongly induce apoptosis not only through replication-dependent p53 overexpression, but also through E1A-dependent enhancement of p53-mediated apoptosis.

The molecular mechanism by which E1A suppresses p53-mediated upregulation of p21 and MDM2 remains unclear. Since adenoviral E1A has been shown to repress the expression of many target genes through activation of p300/CBP [cyclic adenosine monophosphate response element-binding protein (CREB)-binding protein] histone acetyltransferases that cause global histone modification,[33,34] p300/CBP activation may be involved in E1A-mediated p21 and MDM2 suppression. Indeed, E1A-mediated p21 and MDM2 suppression has been shown to be regulated in a p300/CBP dependent manner.[29,31] A recent report also suggested that an E1B-defective adenovirus activates p53 expression, but
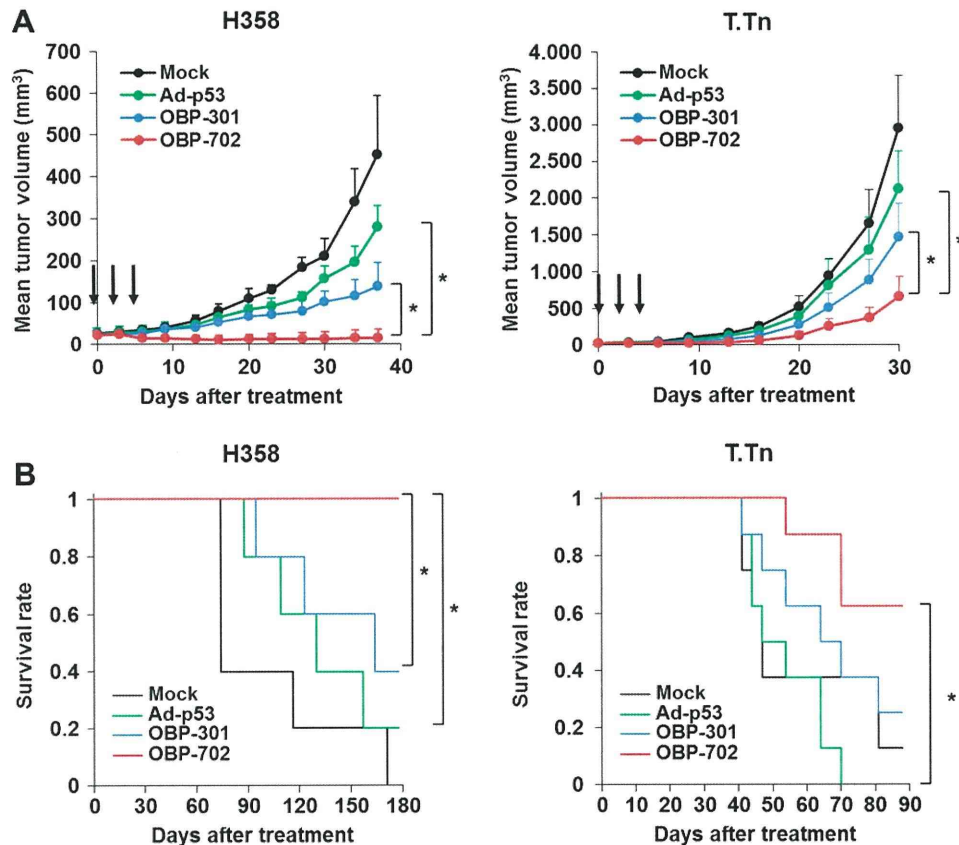
Fig. 5. Strong antitumour effect of OBP-702 on subcutaneous human tumours in xenograft models. (A) H358 or T.Tn cells (5×10^6 cells per site) were inoculated into the flank of 5-week-old female BALB/c *nu/nu* mice. When the tumours reached 3–5 mm in diameter, OBP-702 (10^8 PFU/ tumour), OBP-301 (10^8 PFU/tumour), Ad-p53 (10^8 PFU/tumour) or PBS (Mock) was intratumourally injected on days 0, 2 and 4 (Black arrows). Tumour growth is expressed as the mean tumour volume ± SD in each group of H358 tumours ($n = 5$) or T.Tn tumours ($n = 8$). Statistical significance was determined using Student's *t* test. *$P < 0.05$. The data are representative of three separate experiments. (B) Survival rate in each group of H358 tumours-bearing mice ($n = 5$) or T.Tn tumours-bearing mice ($n = 8$) was shown using the Kaplan–Meier method. Statistical significance was determined using log-rank test. *$P < 0.05$.

suppresses p21 and MDM2 expression, through the binding of E1A with p300/CBP.[35] However, p300 disruption has also been shown to both increase p53 stability through MDM2 suppression, and to suppress p21 expression, resulting in apoptosis in UV-irradiated human cancer cells.[36] Therefore, the role of p300/CBP in adenoviral E1A-mediated p21 and MDM2 suppression may be cell type-specific.

It has recently been shown that siRNA-mediated p21 suppression enhances the antitumour effect of an oncolytic adenovirus,[37,38] suggesting that p21 suppression further induces oncolytic cell death. Oncolytic adenovirus-mediated cell death has been shown to be associated with autophagy-related cell death, which is distinct from apoptosis.[39,40] Autophagy has been shown to be positively regulated by p53,[14] but negatively regulated by p21.[41] These results suggest that p53 upregulation without p21 activation enhances autophagic cell death. Thus, oncolytic adenovirus-mediated p21 suppression may enhance not only p53-mediated apoptosis, but also autophagic cell death during the OBP-702-mediated antitumour effect.

Telomerase-specific replication-competent OBP-301 that possesses the *hTERT* gene promoter replicates, and induces an antitumour effect in, human cancer cells in a telomerase-dependent manner.[9–11] Previous reports have shown that Ad-p53-mediated p53 overexpression suppresses *hTERT* mRNA expression,[42,43] suggesting possible suppression of OBP-301 and OBP-702 replication by p53 overexpression. However, we previously reported that Ad-p53-mediated p53 overexpression did not suppress OBP-301 replication during combination therapy.[24] Shats et al. previously reported that knockdown of p21 eliminated the p53-dependent repression of *hTERT* mRNA expression.[44] Since OBP-702, or combination therapy of OBP-301 with Ad-p53, induces p53 overexpression together with E1A-mediated p21 downregulation, p53 overexpression may not suppress hTERT expression. Furthermore, we recently demonstrated that OBP-301 infection itself induces a 1.1- to 50-fold increase in *hTERT* mRNA expression in an E1A-dependent manner.[45] Thus, OBP-702-mediated p53 overexpression would induce apoptosis without affecting hTERT expression.